UNIFORMED SERVICES UNIVERSITY OF THE HEALTH SCIENCES
F. EDWARD HÉBERT SCHOOL OF MEDICINE
4301 JONES BRIDGE ROAD
BETHESDA, MARYLAND 20814-4799

May 29, 2007

APPROVAL SHEET

Title of Dissertation: "Public Health Implications of the 1540 nm Laser on the Cornea"

Name of Candidate: Nicole McPherson
Doctor of Public Health Degree
30 May 2007

Dissertation and Abstract Approved:

_____   30 May/07
Tzu-Cheg Kao, Ph.D.   Date
Department of Preventive Medicine & Biometrics
Committee Chairperson
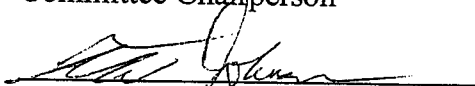
_____   30 may 07
Thomas Johnson, Ph.D.   Date
Department of Preventive Medicine & Biometrics
Committee Member

_____   30 May 2007
MAJ Scott Nemmers, USAF   Date
Department of Preventive Medicine & Biometrics
Committee Member
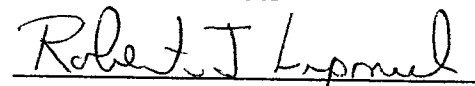
_____   5-30-07
COL Robert Lipnick, USA   Date
Department of Preventive Medicine & Biometrics
Committee Member
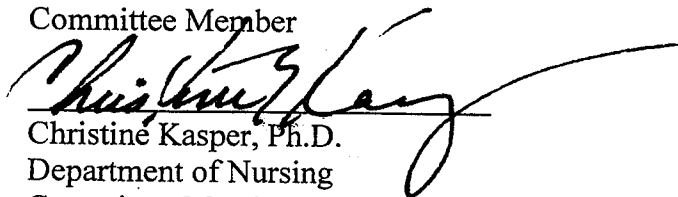
_____   5-30-07
Christine Kasper, Ph.D.   Date
Department of Nursing
Committee Member

The author hereby certifies that the use of any copyrighted material in the thesis manuscript entitled:

"Public Health Implications of the 1540 nm Laser on the Cornea"

is appropriately acknowledged and, beyond brief excerpts, is with the permission of the copyright owner.

Nicole McPherson
Department of Preventive Medicine & Biometrics
Uniformed Services University

ABSTRACT

Public Health Implications of the 1540 nm laser on the Cornea

Nicole A. McPherson, Doctor of Public Health, 2007

Dissertation directed by: Thomas E. Johnson, Ph.D.
Department of Preventive Medicine
and Biometrics

The mid-infrared spectral region is considered to be 'eye safe' due to the unique absorption properties of the cornea. The wavelengths between 1400 and 2000 nm are absorbed by the corneal tissue before they can be focused and injure the retinal portion of the eye. This unique property of the mid-infrared spectrum has lead to numerous applications of lasers. The expanded use of lasers within this spectrum dictates that further research into the bio-effect of the mid-infrared laser be explored. Of particular interest is the 1540 nm laser as it absorption characteristic extends the full thickness of the cornea. Depending on the radiant energy applied this wavelength may cause permanent stromal scarring and necrosis to the endothelial layer of the cornea. This study explored the effects of the 1540 nm laser on three separate corneal models: in-vitro, ex-vivo and in-vivo. The study found the median effective dose to produce an injury was different for the three models, but that a fixed number could correlate the in-vitro and ex-vivo models to the in-vivo model. The study also found that the in-vitro and ex-vivo model's histology was similar to each other and to the in-vivo model except that the in-vivo model showed a proliferative response in the endothelial cells. The

mechanism causing the proliferative response in the in-vivo endothelial cells requires further research to determine if there is a way to use the 1540 nm laser to trigger a proliferation response in human endothelial cells. The thermal response of the in-vivo tissue was also characterized and indicates that further research is required to determine if there is successive heating with serial exposures across the eye.

Public Health Implications of the 1540 nm Laser on the Cornea

by

Nicole A. McPherson

ACKNOWLEDGEMENTS

I would like to thank each member of my committee for all their support and encouragement to make this dissertation possible. I want to thank Dr. Johnson for his tireless effort to make sure we had weekly meeting over the phone to maintain focus on achieving this dissertation. Other people I would like to acknowledge are: Dr. Thomas Eurell for his help and assistance in conducting the histology; Mr Chuck Elliot from the Night Vision Goggle Lab for filming the thermal imagery; and Golda Winston, Tridaugh Winston, Don Randolph, Scott Johanson and Laticia Sanders for assisting in the lab with laser set up, animal care and tissue embedding. I also need to thank Aimee Buelow for her effort on helping me keep my manuscripts in order.

Finally, this dissertation would not have been possible without the love and support of my family. I would not have accomplished this without my husband John's constant encouragement and his drive to see me succeed. I need to thank my children who have had to endure the endless hours of Mommy studying and going to school and wondering when I will be done. For my parents who have had to listen to endless hours of me explaining what I was doing.

Table of Contents

Table of Contents (cont.)

List of Tables

List of Figures

List of Figures (cont)

Chapter 1

Review of the Literature

CHAPTER 1: REVIEW OF THE LITERATURE

1.1 Laser Applications

In 1958, the *Physical Review,* the journal of the American Physical Society, published a scientific paper called *Infrared and Optical Masers,* by Arthur L. Schawlow. This paper is about the invention of the laser, light amplification by stimulated emission of radiation (Schawlow 1969). The paper and the invention of the laser launched a new scientific field and opened the door to numerous applications of the laser. The rate of development and manufacture of lasers is truly phenomenal. Lasers are currently used for a wide range of purposes.

Lasers are used in fiber optics communication, welding, micro machining, cutting, sealing, range finding (hunting and golf), and law enforcement. The medical applications include the use of lasers in LASIK surgery, skin treatments, and in surgery as a soft tissue and bone tissue-cutting device (Markov 2004; Shiner 2004). The military was the first to utilize lasers when Theodore Maiman and his colleagues developed some of the first laser weapon sighting systems (Steen 1998). The military uses lasers for target designation, communications systems, radar warning systems, antiaircraft and antimissile systems, and non-lethal weapons.

These systems pose an eye health risk to personnel exposed indirectly or directly to the laser. The 1500 to 1800 nm wavelength spectral region is safer for the eyes because wavelengths in this band are unable to reach the retina, therefore damage cannot occur in the retina, but can occur in the cornea. The 1540 nm wavelength is therefore considered an "eye safe" wavelength (McCally, Farrell, and Bargeron 1992). The majority of laser

bio-effects researchers study retinal injury because laser damage to the retina results in permanent loss of visual function (SPIE 1995). The first structure of the eye for protection is the cornea, yet it is largely forgotten. Most research dollars spent on laser injury in the DoD are only for threshold research and therefore provide information on only occupational safety. Very little money or research is spent on the medical implications of a corneal infrared laser injury.

The Protocol on Blinding Laser Weapons (Protocol IV to the 1980 Geneva Convention), 13 October 1995 makes the use of blinding laser weapons illegal under international law (ICRC 1995). Yet, there are countries and organizations that employ the laser as a blinding weapon. Jane's Intelligence Review describes the ZM-87 Portable Laser made by China. The weapon, with tripod weighs 73 pounds. The weapon is designed to "injure or dizzy" targeted individuals. The advertised effective range to injure the eye is 2-3 km. When a magnifying optic is utilized the range moves beyond 5 km. The system can also cause short term flaring blindness at rages up to 10 km (Jane's International Defense Review 2005).

In November of 2004, the Federal Bureau of Investigation (FBI) and the U.S. Department of Homeland Security warned pilots of the potential effects of lasers and the threat of overseas terrorist groups expressing an interest in using these devices against human sight. The U.S. National Air and Space Intelligence Center has compiled a classified list of "laser incidents" which numbers more than 50 (Fleischauer 2005). While most laser incidents reported in the past year by commercial airlines dealt with visible spectrum lasers, the use of a non-visible laser, which can cause damage to the eye, would

allow for the terrorist to attack without the pilot being aware and also hinders the ability to determine the location of the attacker.

1.2 Laser Properties

Lasers have specific properties which affect the highly collimated beam's ability to cause injury. The wavelength in nanometers (nm) is specific for each laser and determines what spectral region the laser is operating in. The wavelength determines the beams transmission or absorption characteristics in ocular media. Some wavelengths are only a retinal or a cornea hazard, while some wavelengths are a hazard to both the retina and cornea. The spot size of the beam influences the beams ability to cause injury based off the number of photons that are released in the exposure area. Additionally the pulse duration in seconds (s), the intensity in Joules or Watts (J or W) and the amount of divergence (radians) of the beam all play a role in influencing the beams biological affect on damaging tissue. The properties of the laser beam are taken into account in determining the Maximum Permissible Exposure (MPE) for the laser.

1.3 Laser Standards

There are a number of safety standards that regulate the use of lasers. American National Standards Institute (ANSI) sets industry consensus standards and has published or has under development seven standards specific to the laser field. One standard is the "For the Safe Use of Lasers" (ANSI Standard Z136.1). Some areas of the standard deal with setting and calculating the Maximum Permissible Exposure (MPE), which is based on the Median Effective Dose (ED_{50}). The standard also details engineering designs to protect people from laser hazards as well as required types of personal protective equipment (PPE) and appropriate warning signs (ANSI 2000). Additional ANSI

standards encompass other laser uses: ANSI Standard Z136.2 for fiber optics systems, and ANSI Standard Z136.3 for medical lasers. The ANSI Standard Z136.4 concerning laser measurement is also being developed.

The United States (U.S.) military standards are based on the ANSI standards. The U.S. Navy uses ANSI Standard Z136.1 directly and the Chief of Naval Operations Instructional (OPNAV Inst) 5100.27A "Navy Laser Hazards Control program". The U.S. Air Force has it own standard, the Air Force Occupational Safety and Health (AFOSH) 48-139 - Laser Radiation Protection Program. The U.S. Army uses multiple regulations and technical bulletins such as:

US Army Regulation (AR) 11-9, *The Army Radiation Safety Program*

AR 40-5, *Preventive Medicine*

AR 40-46, *Control of Health Hazards from Lasers and High Intensity Optical Sources*

AR 385-63, Policies *and Procedures for Firing Ammunition for Training, Target Practice, and Combat*

AMC Reg 385-29, *Laser Safety*

TB MED 524, *Control of Hazards to Health from Laser Radiation*

The legal requirements for laser safety include the Title 21 Code of Federal Regulations, Chapter 1040: *Performance Standards For Light-emitting Products*. Some exemptions have been made for the military and are covered under Military Standard (MIL-STD) 1425A (Mil-Std1425A 1991). MIL-STD-882C addresses safeguards from other, related potential hazards(Mil-Std882C 1993). There is also the DoD Instruction

6055.11, "*Protection of DoD Personnel from Exposure to Radiofrequency Radiation and Military Exempt Lasers*."

The government enacted Public Law 90-602 the "Radiation Control for Health and Safety Act of 1968." In 1970 the "Occupational Safety and Health Act" gives attention to the potential effects of non-ionizing radiation in the industrial environment. Environmental laws affect the use of lasers and laser facilities. Congress created the *National Environmental Policy Act of 1969* to establish national policy to protect the environment and to minimize adverse environmental consequences of federal actions (National Environmental Policy Act Of 1973 1973). Certain provisions of the act are incorporated the *Endangered Species Act of 1973 (Endangered Species Act Of 1973 1973).* Many lasers are used outdoors therefore the effect of laser radiation on endangered species and other wildlife must be considered.

The United States is a part of the North Atlantic Treaty Organization (NATO), which maintains a standardization agreement on laser radiation, Standardization Agreement (STANAG) 3606 (NATO 1988). In 1995, the U.S signed the Protocol IV to the 1980 Geneva Convention of Conventional Weapons, the Protocol on Blinding Laser Weapons, and this protocol made the use of lasers as a blinding weapon illegal under international law (NATO 1988).

1.4 Laser Classes

Z136.1 ANSI Standard "For the Safe Use of Lasers" assigns lasers into four classes. The classes are based upon the type of damage the laser can cause. The warning signs are also separated into the four classes.

CLASS 1: Incapable of causing eye damage

CLASS 2: Emit visible light only. Capable of causing eye damage with direct viewing of the beam $\geq$ 0.25s

CLASS 3a: Capable of causing eye damage from short-duration (<0.25s) viewing of the direct beam.

CLASS 3b: Class 3b lasers are capable of causing eye damage from short-duration (<0.25s) viewing of the direct or specularly-reflected beam.

CLASS 4: Capable of causing severe eye damage with short-duration exposure to the direct, specularly-reflected, or diffusely-reflected beam. Capable of producing severe skin damage. May ignite flammable or combustible materials with direct beam. Emits an average radiant power in excess of 0.5 W for >0.25s. This information was adapted from the Z136.1 ANSI Standard "For the Safe Use of Lasers" (ANSI 2000).

1.5 Laser Injuries

Biological hazards of the laser affect the ocular and the dermal tissue. These hazards are based upon the parameters of the laser, as well as the absorption and transmission characteristics of the tissue exposed. In order to determine the extent of biological effects, all the laser parameters must be adjusted and tested. In conjunction with experimental studies, a surveillance reporting system for laser injuries would allow for a human epidemiological study to evaluate the experimental data.

The epidemiological human studies could lead to better injury prevention and appropriate medical treatment of laser injuries that occur. Yet, there is no unified laser injury surveillance reporting system. Even with a system in place, it is likely that the injuries would be underreported due to injuries not properly diagnosed or the injury not considered severe enough to require hospitalization (Clark 2004). For a surveillance

system to work properly, all of the parameters of the laser would be required to compile a useful analysis of the data.

1.6 Eye and Corneal Anatomy

The cornea and the conjunctiva of the eye are both exposed directly to the environment and are protected by the tear film layer. (See Figure 1) The cornea has numerous sensory receptors and nerve endings that serve as the protective reflexes for mechanical and thermal agents (Lasers and optical radiation 1982). The unique structure of the cornea and lack of blood vessels allows the cornea to be clear. The cornea must remain transparent or clear to properly refract light. All layers of the cornea must be free of any cloudy or opaque areas to properly see and refract light. The cornea has 5 distinct layers which are covered by a seven micron tear film layer that helps nourish the cornea (Mishima 1965). (See Figure 2) The corneal tissue is arranged in five basic layers, each having an important function. These five layers are:

Epithelium: The outermost layer is the epithelium. The epithelium acts to block the passage of foreign material from the eye and provide a sooth surface to absorb oxygen and nutrients found in the tear film layer. The epithelium has numerous nerve endings that make the cornea extremely sensitive to pain when an injury occurs. This pain reflex helps protect the rest of the eye from injury. The epithelium has a basement membrane, which acts as an anchor for the epithelium cells.

Bowman's Layer: A strong layer of collagen comprises a transparent sheet of tissue directly below the basement membrane of the epithelium. The Bowman's

layer can form scar tissue as it heals from an injury. If the scars are large enough the vision can be affected.

Stroma: Almost 90 percent of the corneal thickness is comprised of the stromal layer. The stromal layer consists of water and collagen and gives the cornea its strength, elasticity and form. The collagens structure is unique and is essential in the transparency of the cornea. This layer can also form scar tissue which will then affect the vision.

Descemet's Membrane: The Descemet's membrane is also made of collagen fibers, but they are different from the stromal layer collagen. The Descemets membrane is thin, but serves as a protective barrier against infection and injuries. If injured the tissue is easily regenerated from the endothelial cells that lie below it.

Endothelium: The innermost layer of the cornea is only one cell layer thick but essential in keeping the cornea clear. The endothelium layer pumps excess fluid out of the stroma and allows nutrients from the aqueous humor to flow into the stroma. Without proper pumping action of the endothelium the stroma would swell with water, become hazy and opaque. The endothelium cells do not regenerate *in-vivo* if they are lost due to injury or disease. This information was adapted from the National Institute of Health's National Eye Institute (NEI 2007).

The rabbit cornea is very similar to the human cornea, with a distinct difference of having no Bowman's layer. Additionally there are differences in the arrangement of the basement membrane collagen fibers, the presence of small fenestrations in the human posterior stroma keratocytes, the density of the stroma neural plexeus, and the

arrangement of the collagen fibers in the Descement membrane (Ojeda, Ventosa, and Piedra 2001).

1.7 Laser Absorption

The cornea provides protection for the deeper layers of the eye due to the tissue absorbing capability. However this absorptive capability leaves the cornea susceptible to damage (McCally, Farrell, and Bargeron 1992). Different wavelengths of laser radiation are absorbed, reflected, and transmitted by different tissues. The spectral region of 1400 and above is generally considered eye safe because the of the corneas ability to absorb the laser radiation and prevent damaging levels of laser radiation to reach the retina. The spectral region most studied is below 1400 nm due to the energy transmitting through the cornea and focusing on the retinal region and causing possible damage leading to permanent vision loss. (See Figure 3)

1.8 Animals in Research

The live animal model (*in-vivo*) testing is considered the gold standard in determining threshold standards and biological effects of laser exposure. Accepted models for injury to the eye are rabbit, non-human primate, porcine, chicken, and human cadaverous eyes. Currently, the accepted model for human cornea injury is the rabbit (Slatter 1990). While the non-human primate and porcine are also accepted models, there is a greater cost in housing and care required for non-human primates and porcine models.

Rabbits are a well-established model for eye research and rabbit corneas are similar topologically and biochemically to human corneas (ANSI 2000; Ham WT 1991). While

in-vitro models have been developed, they must be evaluated as a replacement model in the injury and healing process.

While the *in-vivo* model is considered the gold standard for testing, the Animal Welfare Act (1966), the Food Security Act of 1985, and USDA Animal Care Policy number 12 have made animal testing requirements more stringent. These requirements have lead to an increased cost in conducting animal experiments. William Russell and Rex Burch introduced the Three R's (Replacement, Reduction, and Refinement) to animal research in their book published in 1959 *The Principles of Humane Experimental Technique* (Russell and Burch 1959). They define the Three R's as:

Replacement: Finding ways to replace animals with non-animals or a lower phylum of animal

Reduction: Reducing the number of animals used in research.

Refinement: Improving the lives of animals used in research by using techniques and procedures that reduce distress and pain

The Three R's have lead researchers to look for alternative models instead of the *in-vivo* animal models (ASPCA 2005). The evaluation of an *in-vitro* and *ex-vivo* replacement models would allow for a reduction in the use of live animals in exploring the eyes physiologic responses to the 1540 nm laser exposure and treatment alternatives, and may eventually lead to a replacement model. Society is placing a social pressure to change from live animal testing, and there are ethical questions raised about using live animals. Research using live animals is expensive due to special facility requirements, personnel, maintenance, occupational health and safety requirements, and the cost of the animal. Alternative models would streamline the monetary and time costs involved in

future laser studies affecting the cornea, allowing researchers to rapidly screen and develop triage and treatment techniques.

1.9 Public Health Impact

While the 1540 nm laser is considered "eye safe" due to the absorption characteristics of the cornea protecting the retinal region of the eye, injury to the cornea can cause severe pain and render a person incapable of working. Injury to the cornea may cause temporary to permanent vision impairment depending on how large of an area is exposed by laser radiation and what layer of the corneal tissue is affected. By understanding the biological effects of the 1540 nm laser, appropriate standards can be set for the MPE and contribute to improvement of occupational health protection for those who work with lasers or may be exposed to laser radiation.

By varying the parameters of laser radiation, injuries may or may not occur with different tissue layers. Using live animals to simulate the biological response to all types of laser radiation, healing and treatment options is not feasible due to time and monetary constraints. By looking at alternative animal models, better assumptions may be made about the effects and response of laser radiation in the corneal hazard region. The evaluation and use of *in-vitro* and *ex-vivo* models allows for a reduction in the number of *in-vivo* or live animals utilized, as well as looking at possible ways to improve these models for future use as replacement models to live animal testing.

While most laser injuries occur in an occupational setting, the current world climate since 9/11 demands that the DOD address force health protection of United States troops and allied forces for laser exposure. While the injuries may still be considered occupational in nature, the effect of losing a soldier on the battlefield is quite different

from losing a worker in an industrial setting. The ocular injury that occurs to a soldier may jeopardize his safety as well as those around him. Current U.S. military doctrine dictates that a soldier be evacuated to rear echelon medical support if life, limb, or eye is in jeopardy of being lost.

If medical personnel are unable to recognize a corneal laser injury, a soldier who may be temporarily down for a few days may be sent to the rear area medical support facility for a minor injury. Once the soldier has recovered it may take numerous days to return the soldier to the unit. If a laser is employed as a non-lethal weapon against our forces, entire units may lose their combat effectiveness just due to temporary vision impairment.

Obtaining experimental data in the corneal hazard region will allow for the characterization of injury and possible treatments available to those affected by laser radiation. Additionally the thermal effects of successive laser radiation exposures in the corneal hazard region should be characterized. Weapons characterized as non-lethal and only causing temporary blindness may in fact be causing permanent vision impairment if successive exposures are occurring.

In addition to occupational and force health protection, homeland security could be affected by the use of laser systems. A terrorist could easily buy or manufacture a laser system to use to interfere with air traffic. A 1540 nm laser would not be visible, but could cause severe pain to a person's cornea. This pain and corneal injury could cause a pilot to have difficulties on making a non-instrument approach for landing and take offs. Understanding how a threat may be employed against our soldiers and our citizens allows for us to combat these efforts and protect ourselves from future terrorist actions.

Table 1: Comparison of Human Eye to Animal Models (Fyffe 2005)

Model	Corneal Diameter	Corneal Thickness	Corneal Epithelium Thickness	Bowman's Layer
Human	11.7 mm	770 um	35 um	Yes
Rhesus Monkey	10.6 mm	460 um	30 um	Yes
Rabbit	10.4 mm	450 um	30 um	No
Porcine	14.2 mm	1063 um	47 um	No
Feline	16 mm	569 um	65 um	No
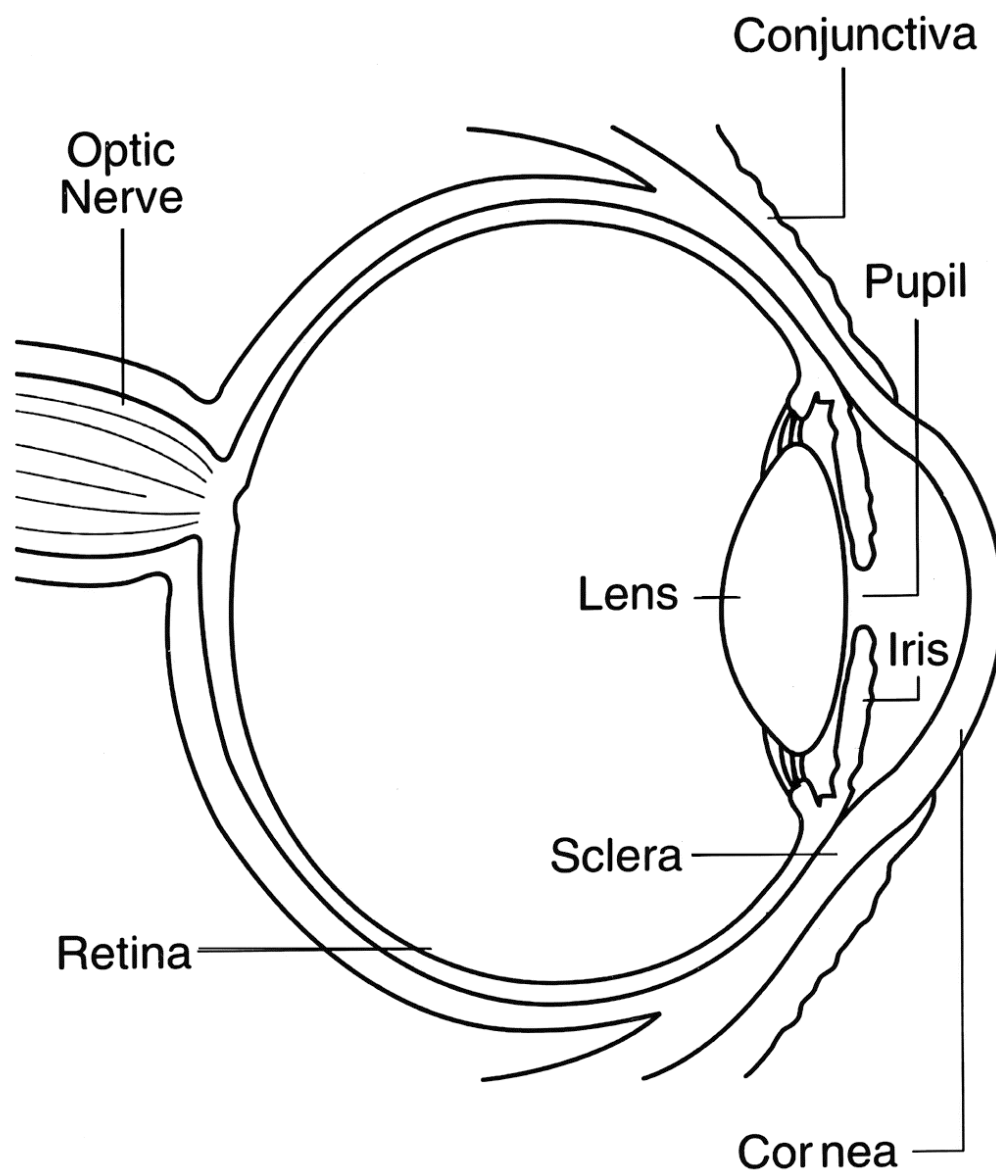
Figure 1: The Structure of the Eye (National Eye Institute, National Institutes of Health

Ref#: NEA05)
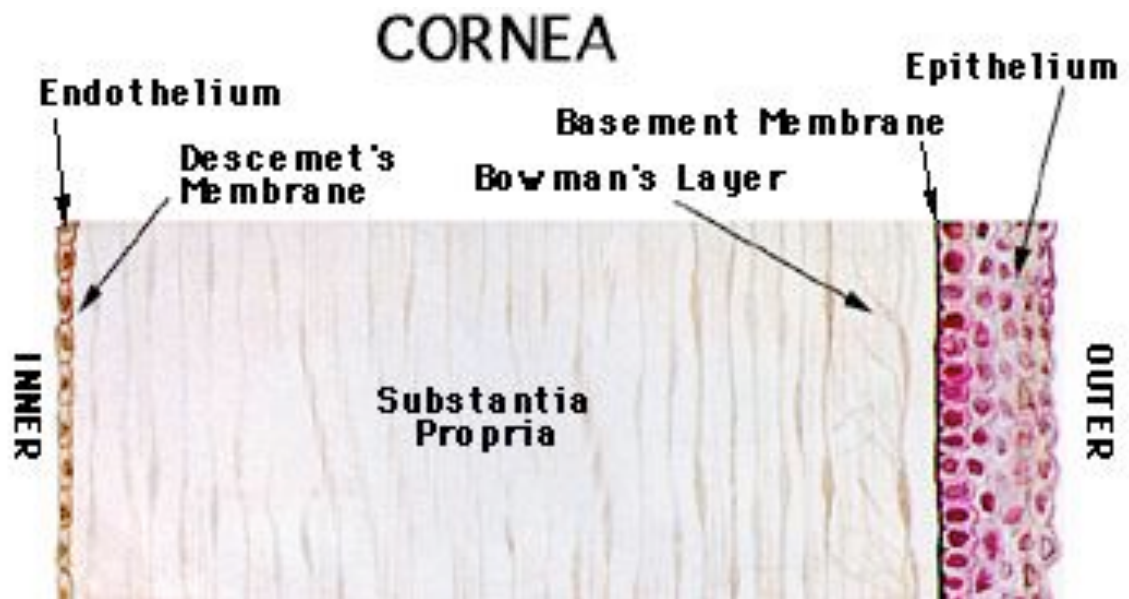
CORNEA

Figure2: The Structure of the Cornea (with permission Leo D. Bores, MD. Ocular

Anatomy: Anterior Segment Anatomy, 2002.

http://www.e-sunbear.com/anatomy_03.html)
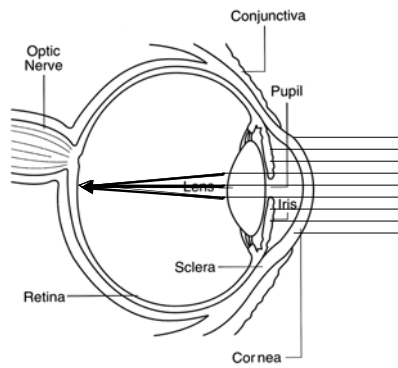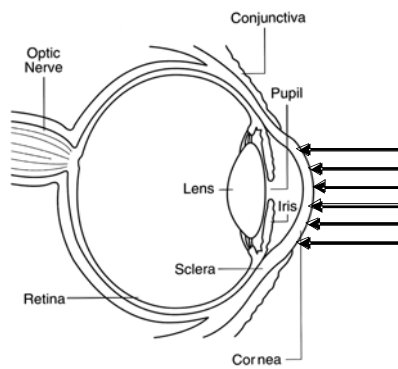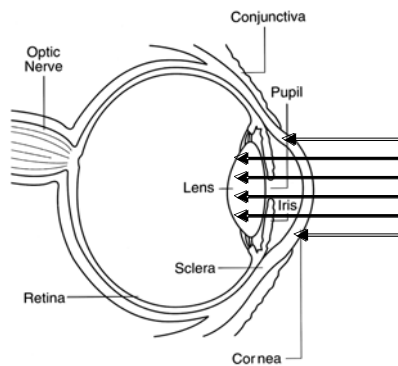
Figure 3: Absorption characteristics of the human eye Adapted from (Sliney and Wolbarsht 1980) and (National Eye Institute, National Institutes of Health Ref#: NEA05)

Chapter 2

Research Methods

CHAPTER 2: RESEARCH METHODS

2.1 Research Objective

To characterize the effects of the 1540 nm laser on the cornea by determining the median effective dose (ED_{50}), morphologic characteristics, and thermal effects.

2.2 Specific Aims

The specific aims to meet the research objective are as follows:

Specific Aim One: Determine the ED_{50} for a visible lesion from exposure to a 1540 nm wavelength laser.

Specific Aim Two: To determine morphologic characteristics of the cornea after exposure to a 1540 nm laser.

Specific Aim Three: To characterize the thermal effects of the 1540 nm laser exposure on the *in-vivo* corneal model.

Specific Aim Four: To determine if successive corneal injury from a 1540 nm laser exposures affects thermal temperature of the *in-vivo* model.

2.3 Study Design and Methods

2.3.1 Overview of Data

Data collection and analysis occurred in support of Dr. Thomas Johnson's USUHS Research Protocol PMB -02-358 "Triage and Treatment of Laser Eye Injury on the Modern Battlefield." The data sets generated are as follows:

1.   Corneal dose response to 1540 nm laser exposure

2.   Thermal imaging of 1540 nm laser exposure to *in-vivo* model

3.   Histological and proteomic analysis of corneal models exposed to 1540 nm laser

2.3.2 Rabbit Animal Model

In-vivo

Dutch Belted Rabbits (Oryctolagus cuniculi) of either sex that weighed between 2-3 kgs were utilized. The Dutch Belted rabbit was utilized due to its brown eye pigmentation, which would aid in grossly visualizing an injury to the cornea. The rabbit is an accepted model for corneal research, is easier and less expensive to maintain than porcine or non-human primate models (Slatter 1990). The rabbit model also has an available *ex-vivo* and *in-vitro* tissue source to reduce the number of live animals utilized in experiments.

The animals involved in this study were procured, maintained and used in accordance with the Animal Welfare Act and the "Guide for the Care and Use of Laboratory Animals" prepared by the Committee on Care and Use of Laboratory Animals of the Institute of Laboratory Animal Resources, National Research Council. The Uniformed Services University of the Health Sciences has been fully accredited by the Association for the Assessment and Accreditation of Laboratory Animal Care, International since 1982.

Ex-vivo

The *ex-vivo* tissue was ordered from a Department of Defense approved tissue source. The tissue was from young rabbits approximately six months in age and the eyes were free from ocular disease. The eyes were enucleated and placed into growth serum and shipped overnight on ice to the laser facility for exposure. The eyes were exposed 18 to 24 hours after enucleating.

In-vitro

Cultures of corneal epithelial cells and keratocytes from rabbit eyes, obtained from rabbits undergoing a terminal procedure and free from ocular diseases, served as the seed cultures for the tissue engineered corneal models. Corneal models were produced in two steps.

First, a liquid collagen/corneal keratocyte seed culture suspension was added to a Transwell (Costar) polycarbonate tissue culture insert contained within a 12-well tissue culture plate. The polycarbonate membrane of the insert served as a platform for the gelatinization of the stromal collagen and the growth of stromal keratocytes. The collagen/ keratocyte suspension forms a gel during incubation (37ºC, 5% CO_2) and the keratocytes were grown in culture for 5-7 days.

Second, a seed culture suspension of corneal epithelial cells was plated upon the collagen/ keratocyte gel and grown in culture for an additional 7-14 days. The tissue culture fluid level was slowly lowered over the incubation period until an epithelial cell-air interface was established. Under optimum culture conditions, the epithelial layer stratifies into basal, wing and superficial cells. One native rabbit cornea will provide the cells necessary to produce approximately 25 tissue engineered corneal models.

2.3.3 Laser

The laser utilized in all the experiments was 0.8 ms pulsed Erbium-Glass Rod Laser with a wavelength of 1540 nm. This laser falls under Class 4 of the ANSI classification system. The beam is Gaussian in nature. The spot size for all exposures ranged from 1.64E-4 cm^2 to 2.16E-3 cm^2. The spot size was determined using a far knife-edge technique described by Siegman (Siegman AE 1991). The exposure diameter was

measured both vertically and horizontally.

A lens, with a focal point of 50 mm, was utilized to focus the laser beam. The corneal tissue was positioned at 54mm from the lens ring. The tissue was exposed outside the focal point of the lens to give a large spot size for better gross visualization of an injury to the cornea. Optical density filters, ranging from 0.1-0.4, were utilized to reduce power applied in the corneal exposures as well as reducing the voltage on the laser, which ranged from 270 to 500V.

2.3.3.1 Laser Set Up

The laser set up was identical for all three corneal tissue models except for the rotation of the *ex-vivo* and *in-vivo* corneal models to account for the curvature of the eye. The *in-vitro* model is flat and therefore did not require rotation to keep the laser exposure perpendicular to the beam. (See Figure 1)

2.3.4 Exposur*e*

The *in-vitro* and *ex-vivo* corneal tissue models were exposed to a 10-pulse marking lesion at the 12-o'clock position. The *in-vivo* model did not receive a laser marking lesion to ensure that the cornea was not perforated. The corneal tissue models all received three single pulsed exposures per eye spaced 2.5 mm apart. This separation keeps the tissue from folding when it is embedded. The known separation also allows for the corneal tissue to be cut more precisely to the center of the lesion giving a better histological analysis of the injury.

2.3.5 Embedding Procedures

The embedding freezing stations were set up according to *Figure 2: Freezing/Embedding Station Layout.* The embedding stations were the same for *in-vitro*, *ex-vivo*, and *in-vivo* experiments.

The freezing dewar has liquid nitrogen and a beaker of hexane inserted into the liquid nitrogen. The liquid nitrogen and hexane is filled to brim of the beaker. The corneal model is removed from the transwell plate. The 5-ml disposable beaker identification were matched to the corneal model transwell palate number. The 5-ml disposable beakers were filled with OCT to about the1/4 level and placed in the freezing bath.

The *ex-vivo* and *in-vivo* corneal models were dissected from the eye globe. The *in-vitro* corneal model was removed from the transwell. The marking lesion was dyed with surgical tissue dye. The surgical tissue dye was allowed a few seconds to dry. A small dot of OCT was placed on the frozen OCT in the 5-ml disposable beaker. All the corneal models were placed epithelium side up on the small dot of OCT with the marking lesion at the 12-o'clock position. *See Figure 3: Disposable Beaker Template and Cornea Placement.*

All the corneal models were allowed to adhere to the dot of OCT and then additional OCT was added to cover the corneal model. The 5ml disposable beaker was placed into the freezing bath. Once the OCT was completely frozen, the 5-ml disposable beaker was removed from the freezing bath and wrapped in foil to prevent the frozen sample from falling out of the 5-ml disposable beaker during shipment. The foil wrapped frozen tissue sample was placed into a Ziploc™ bag marked with the plate identification and placed onto dry ice for overnight shipment for histological analysis.

2.3.6 Data Collection

All exposure data generated was collected in an MS Excel™ spreadsheet denoting the parameters of the laser and the grading for a minimally visible lesion. A digital photo was taken before, immediately post, and 24 hours post exposure. Photos and grading was done in conjunction with treatments. The grading was done by two independent graders and was binary in nature.

The data for the ED_{50} of the *in-vitro*, *ex-vivo* and *in-vivo* cornel models were generated by varying the voltage (V) and using optical density (OD) filters to decrease the number of photons applied to the exposure area. All thermal data was collected in MS Excel™ spreadsheet and by a thermal camera. The thermal images were analyzed for the apparent radiation in degrees Celsius. The thermal images were analyzed to calculate the mean peak temperature difference between the exposure site and a reference point. Temperature differences were calculated before an exposure occurred and post exposure to give a distribution of mean peak temperature change of the *in-vivo* tissue.

Histological data from the exposed corneal tissue was used to characterize the laser exposure. The histological analysis provided depth of damage measured from the center of the exposure site. Since the beam is Gaussian in nature, the center of the exposure site will be the deepest in the tissue. Additionally, the histological analysis looked at new cell proliferation as a way to characterize healing in the corneal tissues. Finally, a proteomic analysis was conducted to determine which proteins were damaged by the laser radiation exposure, and if any proteins were activated in the healing process.

This information aids in the characterization of cellular damage, by describing which cellular layers of the cornea are affected and if vacuoles are formed in the tissues.

2.3.7 Data Analysis

Specific Aim One: Determine the ED_{50} for a visible lesion from exposure to a 1540 nm

wavelength laser.

Probit analysis was utilized to determine the ED_{50}. Probit analysis was developed to

analyze discrete or dichotomous data. This method is used as a statistical tool to

determine the probability of dose-response curves, such as toxicology or threshold studies

for laser safety (Finney 1971). The SAS institute calls the process the Probit Procedure

and it computes the maximum-likelihood estimates of the slope and intercept of the

probit equation. Two goodness of fit chi-square values can be computed using SAS,

Pearson's Chi-square and the Likelihood Ratio Chi-square (Cain CP 1996).

An ED_{50} was calculated for the *in-vitro* and *ex-vivo* corneal models and the *in-vivo*

ED_{50} was previously calculated at 56.0 J/cm^2 (Clarke et al. 2002). The three ED_{50}'s were

compared to determine if they are statistically different from each other.

Null Hypothesis: The ED_{50} of *in-vitro*, *ex-vivo* and the *in-vivo* corneas are the

same.

Alternative Hypothesis: The ED_{50} of *in-vitro*, *ex-vivo* and the *in-vitro* corneas are

different.

Specific Aim Two*:* To determine morphologic characteristics of the cornea after

exposure to a 1540 nm laser.

The histology data for metalloproteinase-2 proliferation in the *ex-vivo* corneal

model was analyzed to look at the distribution of the data and determine the mean for

area of MMP-2. MMP-2 proliferation was used as an indication of healing in an injury.

The *ex-vivo* corneal model the depth of damage at the center of the lesion was analyzed to

determine the mean depth of damage. The mean diameter, depth and area of the lesion was compared using Hematoxylin and Eosin stained tissues to the MMP-2 immunoreaction products to see if there was a difference in the two methods.

Specific Aim Three: To characterize the thermal effects of the 1540 nm laser exposure on the *in-vivo* corneal model.

The thermal image data collected provided an opportunity to establish the mean baseline temperature of the eye before exposure and the mean of the peak delta temperature of Exposure One, Exposure Two, and Exposure Three. Additionally, the mean difference in time (sec) of the peak delta temperature of Exposure One to Exposure Two, and Exposure Two to Exposure Three can be evaluated. This information is utilized in specific aim four to determine if a relationship exists between serial laser exposures in the eye or if the exposures are independent of each other.

Specific Aim Four: To determine if successive corneal injury from a 1540 nm laser exposures affect thermal temperature of the *in-vivo* model.

Correlation is utilized to determine if there is a relationship between Exposure One and Exposure Three peak delta temperature. The three exposures for each eye were analyzed to determine if the corneal tissue heats with subsequent laser exposures.

Null Hypothesis: Successive laser exposure to the eye does not affect the thermal temperature of the *in-vivo* model.

Alternative Hypothesis: Successive laser exposure to the eye does affect the thermal temperature of the *in-vivo* model.
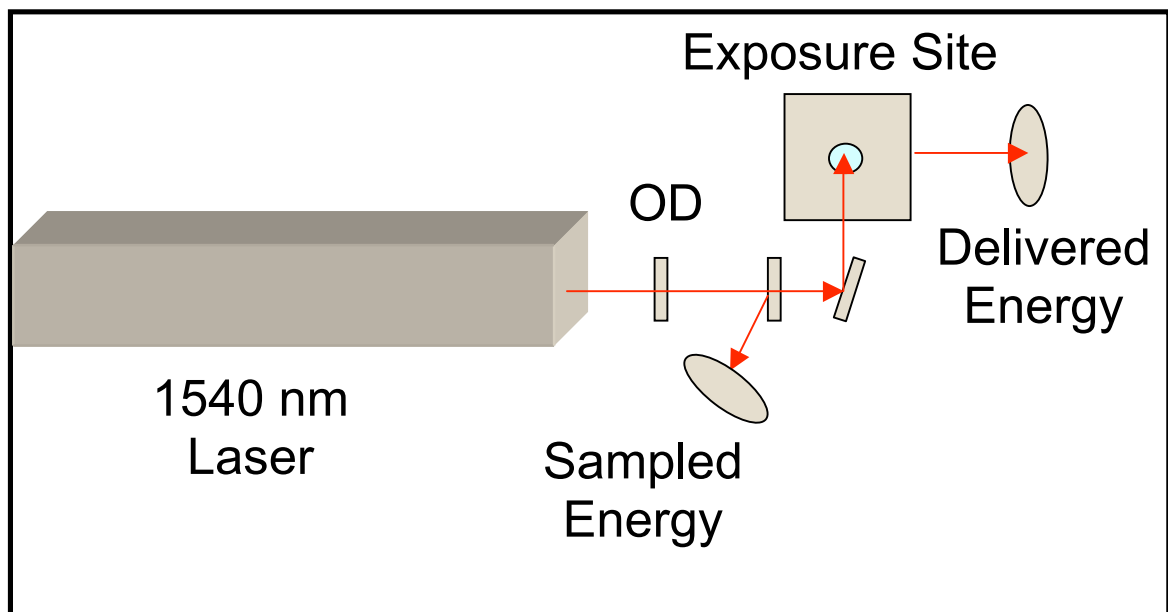
Figure 1: 1540 nm Erbium Laser set up

A. Dewer with Liquid Nitrogen and Hexane Freezing Bath
B. Surgical Station
   a. OCT
   b. Transwell plates
   c. Surgical Dye
   d. 5ml disposable beakers
   e. Tools: needle, razor blades, jeweler forceps, &cornea scissors
   f. Surgical area
   g. 4x4 gauzes
C. Dissecting Light Microscope
D. Dry Ice

Freezing/Embedding Station Two

A

d

a
b
c
e
f
g
B

C

D

Freezing/Embedding Station One
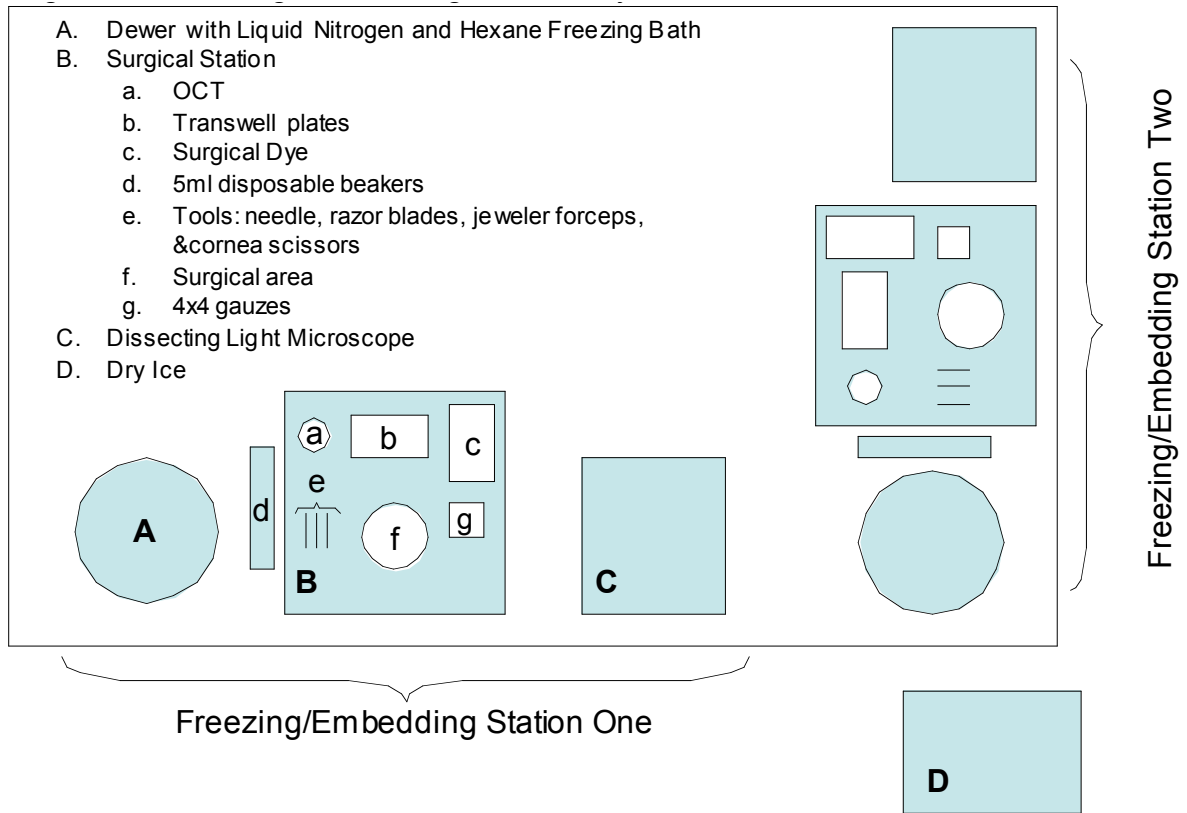
Figure 2: Freezing/Embedding Station Layout
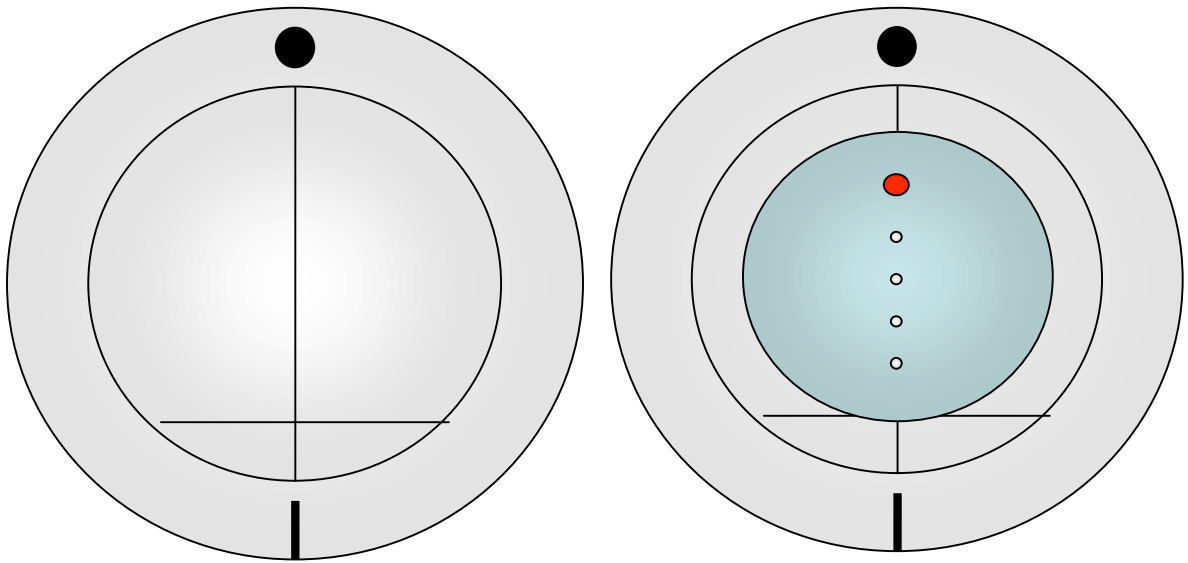
Figure 3: 5-ml Disposable Beaker Template and Cornea Placement

Chapter 3

Results

CHAPTER 3: RESULTS

3.1 Results

      This dissertation is presented in chapters that are largely aligned with the research's specific aims. The research results are documented in four manuscripts presented as chapters (4 - 7) and was written and organized in a manner that would facilitate each chapter's publication in a peer-reviewed journal. The format of this document conforms to the guidelines given in the USUHS "Graduate Student Thesis and Dissertation Requirements Preparation Manual, 10th edition." The peer-reviewed manuscripts are outlined as follows:

1) Comparison of 1540 nm laser induced injuries in *ex-vivo* and *in-vitro* rabbit corneal models (Accepted by the Journal of Biomedical Optics)

2) Morphometric Comparison of the Acute Rabbit Corneal Response to 1540 nm Laser Light Following *Ex-vivo* Exposure to Millisecond and Nanosecond Pulse Widths (Formatted for submission to Journal of Biomedical Optics)

3) Characterization of corneal temperature change in an *in-vivo* (rabbit) model from repeated exposures from a 1.54 micron laser (Formatted for submission to Journal of Biomedical Optics)

4) Case Report: The Potential Hidden Hazards of an OPO Tunable Pumped Laser System (Submitted to Optics and Laser Technology)

Additionally, the following were contributed to as part of this dissertation research but not as peer-reviewed publications:

1) Lab embedding procedures

2) Treatment plans

3) Minor modification to Protocol PMB-02-358

4) Two major modifications to Protocol PMB-02-358

5) Tri-annual review to Protocol PMB –02-358

6) Annual grant report for Grant DAMD17-03-0032

References Cited

ANSI. 2000. *Z136.1-2000 American National Standard For Safe Use Of Lasers* New York: American National Standards Institute.

ASPCA. 2005. Animal Testing: Things Are Changing Because Of New Technology. In *Real Issues*: ASPCA Website.

Cain Cp, Noojin Gd. 1996. *A Comparison Of Various Probit Methods For Analyzing Yes/No Data On A Log Scale*. Usaf Al/Oe-Tr-1996-0102.

Clark, Krystyn. 2004. The Delphi Technique Used In Laser Incident Surveillance, Usuhs.

Clarke, T. F., T. E. Johnson, M. B. Burton, B. Ketzenberger, And W. P. Roach. 2002. Corneal Injury Threshold In Rabbits For The 1540 Nm Infrared Laser. *Aviat Space Environ Med* 73, No. 8: 787-90.

Endangered Species Act Of 1973. 1973.

Finney, D. J. 1971. *Probit Analysis*. Cambridge [Eng.]: University Press.

Fleischauer, Eric. 2005. Blinding Light As A Weapon: Lasers Pose Threat To Airplane Pilots *Decatur Daily News*, Jan 7 2005

Fyffe, James. 2005. Corneal Injury To Ex-Vivo Eyes Exposed To A 3.8 Micron Laser, USUHS.

Ham Wt, Mueller Ha. 1991. Ocular Effects Of Laser Infrared Radiation. *J. Laser App* 3, No. 3h: 19-21.

ICRC. 13 October 1995 1995. *Protocol On Blinding Laser Weapons (Protocol Iv To The 1980 Geneva Convention)*. United Nations Ccw/Conf.I /7. Accessed 1 September 2005. Available From

Http://Www.Icrc.Org/Ihl.Nsf/0/49de65e1b0a201a7c125641f002d57af?Opendocu
ment.

Jane's International Defense Review. 2005. Jane's.

Lasers And Optical Radiation. 1982. In *International Programme On Chemical Safety
Environment Health Criteria 23*:40: The United Nations Environment Programme, The
International Labour Organisation, And The International Radiation Protection
Association.

Markov, Vladimir. 30 Sep 04. 2004. *Eye-Safe Ladar Laser Transmitter*. Navy. Accessed
8 May 2007. Abstract. Available From
Http://Www.Dodsbir.Net/Selections/Abs011/Navyabs011.Htm.

McCally, R. L., R. A. Farrell, And C. B. Bargeron. 1992. Cornea Epithelial Damage
Thresholds In Rabbits Exposed To Tm:Yag Laser Radiation At 2.02 Microns.
Lasers Surg Med 12, No. 6: 598-603.

Mil-Std882c. 1993. Systems Safety Program Requirements, Ed. Dod, Military Standard
882c: Us Department Of Defense.

Mil-Std1425a. 1991. Safety Design Requirements For Military Lasers And Associated
Support Equipment, Ed. Dod, Military Standard 1425a: Us Department Of
Defense.

Mishima, S. 1965. Some Physiological Aspects Of The Precorneal Tear Film. *Arch
Ophthalmol* 73: 233-41.

National Environmental Policy Act Of 1973. 1973.

NATO. 1988. Evaluation And Control Of Laser Hazards On Military Ranges., Mons, Belgium: Nato Standardization Agreement (Stanag) 3606: North Atlantic Treaty Organization.

NEI. 2007. *Facts About The Cornea And Corneal Disease*. Accessed 15 August 2005. Website. Available From Http://Www.Nei.Nih.Gov/Health/Cornealdisease/Index.Asp#0.

Ojeda, J. L., J. A. Ventosa, And S. Piedra. 2001. The Three-Dimensional Microanatomy Of The Rabbit And Human Cornea. A Chemical And Mechanical Microdissection-Sem Approach. *J Anat* 199, No. Pt 5: 567-76.

Russell, W. M. S. And R. L. Burch. 1959. *The Principles Of Humane Experimental Technique*. Springfield, Ill.,: C.C. Thomas.

Schawlow, Arthur L. 1969. *Lasers And Light; Readings From Scientific American*. San Francisco,: W. H. Freeman.

Shiner, Bill. 2004. Fiber Frenzy. In *Industrial Laser Solutions*

Siegman Ae, Sasnett Mw, Johnston Jtf. 1991. Choice Of Clip Levels For Beam Width Measurements Using Knife-Edge Techniques. *Ieee J Quantum Electron* 27: 1098-1104.

Slatter, Douglas H. 1990. *Fundamentals Of Veterinary Ophthalmology*. Philadelphia, Pa: Saunders.

Sliney, David H. And Myron Wolbarsht. 1980. *Safety With Lasers And Other Optical Sources : A Comprehensive Handbook*. New York: Plenum Press.

SPIE. 1995. SPIE Milestone Series: Selected Papers On Laser Safety, Ed. Brian J. Thompson And David H. Sliney, Ms 117 SPIE Optical Engineering Press.

Steen, W. M. 1998. Brief History Of Laser. In *Laser Materials Processing*, 2nd Ed. :
University Of Liverpool.

Chapter 4

Comparison of 1540 nm laser induced injuries in *ex-vivo* and *in-vitro* rabbit corneal

models.

Comparison of 1540 nm laser induced injuries in *ex-vivo* and *in-vitro* rabbit corneal models.

Nicole A. McPherson [1], Thomas E. Eurell [2*], Thomas E. Johnson [2]

Nicole A McPherson, MPH; Uniformed Services University of the Health Sciences, Bethesda, MD, 20814 Nmcpherson@usuhs.mil [1]

Thomas E. Eurell, DVM, PhD; Colorado State University, Fort Collins, CO, 80523 Thomas.Eurell@colostate.edu [2]

Thomas E Johnson, PhD; Colorado State University, Fort Collins, CO, 80523 Thomas.E.Johnson@colostate.edu [2]

Correspondence should be directed to Dr. Thomas E Johnson*
Colorado State University
1618 Campus Delivery
Fort Collins, CO 80523
Phone 970-491-0563
Fax 970-491-0623
Thomas.E.Johnson@colostate.edu

Abstract

Despite the increasing use of infrared lasers in medical, industrial and military settings, data on threshold radiant exposures and median effective dose (ED_{50}) as they relate to laser-tissue interaction are limited. The goals of the present study were to determine the ED_{50} for single-pulse, 1540 nm laser exposures in *ex-vivo* and *in-vitro* rabbit corneal models and characterize the histopathological changes associated with the laser-tissue interaction. An Erbium-Glass laser was used to deliver single, 1540 nm wavelength pulses to 27 *ex-vivo* and 24 *in-vitro* rabbit corneal models. The *ex-vivo* model was exposed to single pulses of 0.8 ms duration and radiant energies ranging from 17.61 J/cm^2 to 42.26 J/cm^2. The *in-vitro* corneal models were exposed to single pulses of 0.8 ms duration and had radiant exposures ranging from 14.87 to 29.72 J/cm^2. Tissue exposure sites were observed for presence of a lesion immediately post exposure and 24 hours after exposure. Histopathological evaluations of tissue exposure sites were conducted 24 hours after exposure. The ED_{50} was determined to be 21.24 J/cm^2 for the *in-vitro* rabbit corneal models and 30.86 J/cm^2 for the *ex-vivo* corneal models. Both the *in-vitro* and *ex-vivo* models displayed similar histopathological responses of tissue necrosis and epithelial cell proliferation.

Keywords: Infrared laser, eye safe, tissue culture, ED_{50}

Introduction

Lasers are common in everyday life and can be found in a variety of devices including range finders, scanners, printers, welding tools, fiber optics, and medical instruments. While science, medicine and society in general have enjoyed the benefits of lasers, there are also inherent ocular safety issues that should not be overlooked. Awareness of these dangers has fostered the use of lasers operating in the 1400 to 2200 nm region,[1,2] since these wavelengths are absorbed by the cornea and anterior chamber before they can cause permanent damage to the retina. However, this approach is not without risk. The cornea has a high density of pain receptors, so even small amounts of damage can cause severe pain.[3,4] The cornea provides approximately 85% of the focusing power in the eye,[5] so laser-induced damage that alters corneal shape or transparency can have a pronounced effect on vision.

The majority of studies reported to evaluate laser eye injuries and ocular safety issues rely on *in-vivo* laser exposures of experimental animals.[6] The maximum permissible exposure (MPE) recommendation currently listed in the ANSI standards for 1540 nm is specifically based on median effective dose (ED_{50}) data derived from *in-vivo* exposures of non-human primate corneas to Erbium lasers.[7] However, the literature provides several different ED_{50} values for the 1540 nm laser that range from 4.7 to 56 J/cm^2.[7-10] This difference has been suggested to correlate with pulse duration and the dependence on the spot size of the laser beam.[11]

Rabbits are a well-established, non-primate, *in-vivo* model for human eye research and a robust database exists for laser-induced corneal injury in rabbits.[10, 12-15] However, in

order to reduce the number of experimental animals used in potentially painful studies, researchers continue to look for alternatives to traditional *in-vivo* animal models.[16-18] Alternative testing methods such as those using ***ex***-*vivo* or *in-vitro* tissues support the concept of reducing painful experimental procedures while allowing researchers to rapidly screen treatment techniques and develop safety standards for ocular laser exposure.

The purpose of the present study was to determine the ED_{50} of 1540 nm laser-induced injuries in *ex-vivo* and *in-vitro* rabbit corneal models and compare the immediate and 24 hours post-exposure tissue responses. Because of the correlation between ED_{50}, pulse duration and laser beam spot size, the present study used analogous laser parameters to those reported by Clarke et al. for *in-vivo* exposure of rabbit eyes to 1540 nm laser light.[10]

Methods

Laser system

An Erbium-Glass laser (Laser Sight Technologies, Winter Park, FL) producing 0.8 ms pulses at 1540 nm was used for all *in-vitro* and *ex-vivo* exposures. The laser is a free running, optically pumped system, with pulse shapes that are roughly Gaussian. The laser beam was focused with a 50 mm lens (BK-7 lens material, LA1708, Newport, Irvine CA) and the spot size was determined using a knife-edge technique.[19] Laser energy was measured with a Molectron EPM-2000 meter and a J25 energy detector (Coherent, Santa Clara, CA). Pulse duration was measured using a Germanium photon detector (PDA 255, Thor Labs, Newton, NJ) connected to a Tektronix TDS 644B digitizing oscilloscope

(Beaverton, OR). The epithelial surfaces for both *in-vitro* corneal tissues and ***ex-vivo***
eyeballs were positioned at a distance of 54 mm from the lens.

Ex-Vivo Rabbit Corneal Model

Rabbit eyes for the *ex-vivo* experiments were provided in a single shipment from
a commercial source (Pel-Freeze, Rogers, AR). All eyes were obtained from rabbits
approximately 6 months of age and shipped overnight, on wet ice, in bottles containing
0.1M phosphate buffer, pH 7.2 supplemented with 1% fresh rabbit serum, 100 IU/ml
penicillin, 100 μg/ml streptomycin and 0.25 μg /ml amphotericin.. Eyeballs that showed
corneal opacity after shipment were excluded from the study. A total of thirty-one eyes
were used for this study. There were four control eyes which were handled in the same
way as the exposed eyes except for laser exposure. The corneas from twenty-seven eyes
were exposed in four locations (1 marking lesion and 3 experimental, see laser exposure
parameters below) for a total of 108 exposures. The *ex-vivo* corneal models were
maintained in an incubator at, 37 $^{\circ}$C and 5% CO_2 immediately prior to exposure and post-
exposure. This approach was taken to mimic the natural environment of the *in-vivo*
cornea where the optical absorption characteristics of the tissue are temperature
dependent.[20] After laser exposure, each eye was placed in a separate well of a 12 well
plate and incubated with F12/DMEM media (MediaTech) supplemented with 10%
NuSerum (Collaborative Biomedical), 2 mM L-glutamine, 100 IU/ml penicillin, 100
μg/ml streptomycin and 0.25 μg/ml amphotericin for 24 hours at 37°C and 5% CO_2 to
evaluate the tissue response to laser injury. The eyes were moved by grasping the optic
nerve with forceps to ensure the cornea was not injured during handling.

In-vitro Rabbit Corneal Model

Primary corneal epithelial cells and stromal keratocytes isolated from New Zealand White rabbits served as the seed cultures for the *in-vitro* corneal models. All cell culture procedures were conducted using F12/DMEM media. Corneal equivalents were produced in two steps.[21] First, a liquid collagen/corneal keratocyte seed culture suspension was added to a Transwell (Costar) tissue culture insert, with a porous polycarbonate supporting membrane, contained within a 12 well tissue culture plate. The collagen/ keratocyte suspension formed a gel during incubation (37°C, 5% CO_2) that was supported by the polycarbonate membrane and the keratocytes were grown in culture for 5-7 days. Second, a seed culture suspension of corneal epithelial cells was plated upon the collagen/ keratocyte gel and grown in culture for an additional 14-21 days. The tissue culture fluid levels were slowly lowered over the incubation period until an epithelial cell-air interface was established that allowed stratification of the epithelial layers into basal, wing and superficial cells.

A total of 24 *in-vitro* rabbit corneal models were used for this study. Four corneal models were used as controls, and twenty corneal models were exposed in four locations (1 position marker and 3 experimental, see laser exposure parameters below) accounting for 80 exposures. The *in-vitro* corneal models were maintained in an incubator at, 37 ^{o}C and 5% CO_2 immediately prior to exposure and post-exposure in a manner analogous to the *ex-vivo* corneal models. After laser exposure, each corneal model was placed in a separate well of a 12 well plate and incubated with F12/DMEM media for 24 hours at 37°C and 5% CO_2 to evaluate the tissue response to laser injury.

Laser Exposure Parameters

The spot size and calibration factor were calculated for each input energy voltage. Ten pulses were used to create a positional marking lesion at the edge of the *in-vitro* and *ex-vivo* corneal models. This marking lesion provided a reference point for histological analyses. The first experimental exposure was made using a single pulse, exactly 2.5 mm from the marking lesion. Two successive single pulse exposures were spaced exactly 5 mm and 7.5 mm from the marking lesion (Fig. 1). Because of the curvature of the cornea in the *ex-vivo* model, the placement of the lens relative to the corneal surface was adjusted for each exposure to maintain a constant 54 mm distance. The *in-vitro* corneal model was flat and received a consistent spot size and shape for all experimental exposures without continuous adjustment.

Evaluation for Injury

All experimental laser exposure sites were independently evaluated within 1 minute post-exposure and 24 hours post-exposure by two graders. Exposure site examinations were conducted with and without the aid of a handheld ophthalmoscope (Welch Allyn, Skaneateles Falls, NY). Lesions were graded on a nominal scale of present or absent, based on agreement by both graders. Fluorescein staining (Fluor-I-Strip®-AT, 9 mg strips, Bausch & Lomb, Rochester, NY) of *ex-vivo* exposure sites was evaluated with a woods lamp and used to highlight laser lesions. Fluorescein staining was not necessary and not used to highlight laser lesions with *in-vitro* exposure sites. The *ex-vivo* corneal models were rinsed with sterile water after fluorescein application to reduce background

staining. All corneal models were photographed before laser exposure, within 1 minute post-exposure, and 24 hours post-exposure using a Nikon D1H digital camera with an F-50 Nikon macroscopic lens (El Segundo, CA). After grading and photography, each corneal model was placed into an individual well of a 12-well culture plate containing F12/DMEM media and incubated for 24 hours at 37°C and 5% CO_2. After the 24 hours post-exposure incubation, the corneal models were removed, graded and photographed for presence or absence of a visible lesion.

Embedding and Freezing of Corneal Tissues for Histological Evaluation

The corneas were recovered from the *ex-vivo* models by sharp, circumferential dissection at the limbal margins. The *in-vitro* corneal models were entirely removed from the transwell by sharp dissection of the underlying polycarbonate membrane. The marking lesion on each corneal tissue was highlighted using a surgical dye to facilitate positioning within the embedding matrix. Each corneal tissue was placed into a 5 ml disposable beaker filled with cryotome embedding medium (OCT, Sakura FineTech, Torrance, CA) and oriented with the marking lesion at the 12 O'clock position and subsequent lesions along the centerline. The corneal tissues were then placed in a freezing bath of hexane surrounded by liquid nitrogen. Once frozen the 5 ml disposable beaker was removed, covered with aluminum foil, placed into a labeled cryostorage bag and stored at -80°C until processed for histology.

Histology

Tissue sections were made using a motorized cryomicrotome (Bright Instruments, Huntingdon, England). The tissues were rapidly trimmed in the cryomicrotome until the highlighted marking lesion was revealed. The micrometer on the cryomicrotome was then set and the tissues trimmed to reveal the exposure sites that were exactly 2.5 mm apart. The marking lesion and the exact spacing of the exposure sites allowed sectioning of the lesions with micrometer precision and accurately resolved the inside edge, middle and outside edge of the laser lesion. Sections to be evaluated for histopathology were stained using Gill's #3 Hematoxylin for 30 seconds, rinsed in tap water for 5 minutes and counterstained using Eosin/Phloxine for 30 seconds. Stained sections were then be dehydrated in a series of alcohols, dipped in xylene and mounted using Eukitt (Electron Microscopy Services, Hatfield, PA). Images for histopathological analyses were captured using a Leitz Orthoplan microscope equipped with a SpotRT digital camera (Diagnostic Instruments, Sterling Heights, MI). Criteria used to evaluate the tissue responses to laser exposure included alterations in the epithelial parameters (e.g., area of hyaline coagulative change vs. area of granular coagulative change) and stromal parameters (e.g., area of coagulative necrosis, number and distribution of keratocytes). Comparisons were made between treatment groups and control groups to evaluate the 24 hours post-exposure healing response.

Statistical Analysis of Laser Lesions

A Probit statistical model was used to determine the ED_{50} for all stochastic injury results.[22,23] The SAS 9.1 Probit Procedure (SAS. Inc., Cary, NC) was used to determine the ED_{50} with 95% fiducial intervals, as well as a χ^2 value. The goodness-of-fit test for the

predicted data was determined using the Pearson's chi-square and likelihood ratio chi-square. If the Pearson goodness-of-fit chi-square test was applied and the *p*-value for the test was too small, a heterogeneity factor and a critical value from the *t* distribution were used to compute the fiducial limits. If the injuries followed a deterministic pattern, the technique described by McCally was utilized to determine the threshold of injury.[24]

Results

Laser Parameters

The laser produced an exposure spot size range of 2.62E-03 cm^2 to 3.16E-03 cm^2 at a distance of 54 mm above the epithelial surface of the rabbit corneal models. The spot size was oval in shape with diameters ranging from 0.582 x 0.572mmto 0.660 x 610mm respectively. The pulse duration was 0.8 ms. The *ex-vivo* corneal models had radiant exposures ranging between 17.61 and 42.26 J/cm^2. The *in-vitro* corneal models had radiant exposures ranging between 14.87 and 29.72 J/cm^2 (Table 1).

Ex-Vivo Rabbit Corneal Models

Analysis of the data using the probit statistical method yielded an ED_{50} of 30.86 J/cm^2 for the immediate post-exposure observations and an ED_{50} of 32.41 J/cm^2 for the 24 hours post-exposure observations (Table 1). The Pearson chi-square and the log-likelihood ratio chi-square tests were not significant at the 0.1 level for the immediate *ex-vivo* corneal model data. The immediate post exposure *ex-vivo* corneal model Type III analysis of effects for the dose gave a Wald chi-square of 11.95 and a p-value of 0.0005.

The *ex-vivo* corneal models had 42 lesions out of 75 exposures apparent immediately after exposure. All lesions were clearly identified immediately after

exposure except for one exposure at 33.04 J/cm^2 which only had a visible lesion at the 24-hour examination.

The lesions produced immediately after laser exposures were clearly visible with no disagreement between graders. The lesions appeared as circular, discrete, raised, opaque, white areas on the cornea (Fig. 2). Use of the ophthalmoscope and fluorescein staining did not reveal any lesions that were not visible with careful gross examination, although these aids did provide better detail of the lesion border. After 24 hours of incubation, the gross appearance of the *ex -vivo* lesions remained as circular, discrete, raised, opaque, white areas on the cornea. Histological analyses of tissues 24 hours post-exposure revealed both tissue necrosis and a proliferative response (Figs. 3 & 4).

The *ex-vivo* corneal model's immediate ED_{50} fell within the 95% fiducial limits of the 24 hours ED_{50}, indicating that the two ED_{50}'s were not significantly different and the ED_{50} could be taken immediately post-exposure instead of waiting 24 hours to determine the threshold (Table 1).

In-Vitro Rabbit Corneal Model

Probit analysis was not used to evaluate the *in-vitro* corneal models because the data was deterministic. McCally's technique to determine the threshold was applied.[24] The threshold exposure was defined as the midpoint energy between where the laser produced a minimal lesion and had no observable effect. Radiant exposures below 20.59 J/cm^2 did not produce a visible lesion, even when viewed using the ophthalmoscope, while all exposures over 21.89 J/cm^2 produced a visible lesion. The data did not change for the immediate vs. 24 hours post-exposure; therefore, the threshold exposure was 21.24 J/cm^2.

All lesions appeared immediately after laser exposure and were clearly visible (without fluorescein staining) with no disagreement between graders (Fig. 2). Fluorescent staining was not useful in the *in-vitro* model as the entire tissue was dyed pale yellow.

The lesions appeared as discrete holes in the tissues. There was no color change in the tissue. Lesions did not appear to change grossly after the 24-hour post-exposure incubation. Histological analyses revealed both tissue necrosis and a proliferative response (Figs. 5 & 6).

The *in-vitro* corneal model ED_{50} of 21.24 J/cm^2 was not within the *ex-vivo* corneal model's ED_{50} 95% fiducial limits of 29.49 - 32.03 J/cm^2 indicating the two ED_{50}'s were different from each other (Table 1). Yet, the two models showed similarity in their histopathological responses with tissue necrosis and epithelial cell proliferation.

Discussion

The *ex-vivo* and *in-vitro* corneal models allow for alternatives to the gold standard *in-vivo* model when exploring damage thresholds for the infrared wavelengths. The *ex-vivo* and *in-vitro* corneal models exposed to the 1540 nm wavelength also provide new data to aid in the determination of the infrared laser safety MPE. These models have certain benefits and disadvantages. Both the *in-vitro* and *ex-vivo* model's median effective dose thresholds are different from the thresholds reported for *in-vivo* laser exposures in rabbits using analogous exposure conditions.[10] The *in-vitro* model uses far less animals to produce the corneal models for experimentation, but the model takes time to produce and requires personnel and equipment for cell culturing. The *ex-vivo* tissue model uses the same number of animals, but the globes may be obtained through tissue sharing or from approved tissue sources and the number of animals experiencing pain

during experimental procedures is reduced. The *in-vitro* corneal model allows for exact

spot size duplication while moving the exposures along a horizontal axis due to the

flatness of the tissue. This is important as it reduces the time to expose the tissue,

compared to the *ex-vivo* tissue, and ensures reproducibility for each exposure point. Both

models allow researchers without lab animal facilities to conduct laser tissue experiments

more readily.

The *in-vitro* and *ex-vivo* corneal models were incubated for 24 hours to encourage

healing but only the *ex-vivo* corneal model showed a change in the number of grossly

visible lesions after 24 hours and subsequently a change in the ED_{50}. This change in the

ex-vivo ED50 was not significant. While the grossly visible changes in the *ex-vivo* model

were not seen in the *in-vitro* model, histology revealed a different picture, with both

models showing a proliferation of the epithelial cells, indicating a healing process was

initiated.

The ED_{50} of both the *ex-vivo* and *in-vitro* models were much higher than the ED_{50}

that was reported by Avdeev, Lund and Stuck for the 1540 nm laser.[7-9] We propose that

this difference is related to the spot size and pulse duration of the laser beam. The spot

size reported by Avdeev, Lund and Stuck ranged from 1-2 mm in diameter. The beam

spot size determined in the present study was oval in shape and ranged from 0.582 to

0.660 mm in diameter, similar to Clarke's work where the diameter of the beam was

0.418x0.598mm. McCally reported that both spot size and pulse duration affect the

median effective dose for the 1540 nm wavelength. He also reported that at shorter pulse

durations the 1540 nm laser does not follow a modified critical temperature model.[11]

Both the *in-vitro* and the *ex-vivo* ED_{50}'s determined in the present study were well below the ED_{50} of 56.0 J/cm^2 reported for analogous *in-vivo* infrared laser exposures[10] This increased sensitivity of the model systems may be useful in rapid screening of laser-tissue interactions but should be taken into account when extrapolating experimental data. Since the biological effects of laser exposure depend on tissue chromophores and the absorption properties of the exposed tissue, the higher *in-vivo* ED_{50} most likely indicates differences in the structural and chemical characteristics of the corneal models compared to the living native tissue.

Factors that could contribute to the elevated threshold for laser injury following *in-vivo* exposures would include: the thickness and composition of the tear film layer, the relative deturgescence of the cornea and the homoiothermic temperature of the tissue.[25] The tear film layer provides nutrients to the cornea and the different nutrients may contain chromophores that alter the laser energy before being absorbed by the corneal tissue. The inherent light absorbing characteristics of the corneal models and the native tissue may also differ. An obvious difference is the coloring of the three tissues. The *in-vivo* exposure data were reported using Dutch Belted rabbits[10] which have a dark brown iris, while the *ex-vivo* models in the present study used a New Zealand White rabbit with a pink eye, and the *in-vitro* model was light pink throughout. The different coloring of the three models may affect the laser absorption and influence the laser damage threshold.

Finally, ***in-vivo, ex-vivo*** and ***in-vitro*** ocular systems have inherently different levels of tissue complexity which may be reflected in the complexity of the tissue chromophores. The *in-vivo* tissue would have the most complex system as it gains

nutrients from both the tear film layer and the aqueous humor, which are dynamic systems. The *ex-vivo* would be less complex and the *in-vitro* the least complex.

The *in-vitro* and *ex-vivo* ocular tissues appear not to have an overlap of fiducial limits, indicating a significant statistical difference in the ED_{50}. This statistical difference cannot be explained by spot size or pulse duration because these laser parameters were held constant during the study and most likely is related to inherent differences between the model tissues. However, there is a relationship between the data from the in-*vitro and ex-vivo* models used in the present study and the *in-vivo* data reported by Clarke et al. that should provide a method to extrapolate *in-vitro* and *ex-vivo* data to predict the response of *in-vivo* exposures. We determined that the *in-vivo* ED_{50} reported by Clarke et al. is approximately 2.64 times that for the *in-vitro* corneal model and 1.81 times that for the *ex-vivo* corneal model (Table 2).[10]

The tissue reaction in the first 24 hours post-exposure appeared to primarily involve the epithelial cells. The histopathological response of the *in-vitro* corneal tissue was analogous to the response of the *ex-vivo* rabbit corneas with essentially identical nuclear and cytoplasmic patterns of coagulative necrosis. The marked epithelial proliferation observed with the *in-vitro* model was primarily restricted to the cells of the *stratum basale* in a similar manner as observed with the *ex-vivo* tissue. These results indicate that, from a histopathological perspective, the *in-vitro* rabbit corneal tissues developed in the present study are appropriate models for the acute post-exposure response of native corneal tissue following 1540 nm laser exposure. In addition, we believe this is the first report of acute, post-exposure corneal epithelial cell proliferation induced by single-pulse, 1540 nm laser light.

The histopathological responses of the *ex-vivo* and *in-vitro* corneal models appear to bracket the histological observations reported by Clarke et al in a manner that may reflect the radiant exposure deposition and highlights an increased sensitivity of the *in-vitro* model to radiant exposure. The representative histological image shown in Clarke's publication revealed a full thickness stromal response 24 hours following a single, 1540 nm and 0.8ms pulse with a radiant exposure of 145 J/cm^2. The *ex-vivo* model used in the present study showed only a small stromal effect with a radiant exposure of 37 J/cm^2 (Fig. 3). The *in-vitro* model used in the present study showed a total ablation of the stromal matrix within the beam field with a radiant exposure of 28 J/cm^2 (Fig. 5).

The combination of a fixed factor that can be applied to *in-vitro* and *ex-vivo* experimental data and the similarity of the histopathological response between *in-vitro* and *ex-vivo* corneal models will improve the extrapolation of experimental data to *in-vivo* results and help fill in the gap of research data appropriate for infrared laser safety standards. In addition, the apparent increased sensitivity of the *in-vitro* model to laser effects (supported by ED_{50} and histopathological observations) may help detect subtle laser-tissue interactions.

Acknowledgements

Table 1: Median Effective Dose and Fiducial Limits of Tissue Response by Experimental Model.

Model	ED$_{50}$ (J/cm^2)	95% Fiducial Limits	
		Lower Limit	Upper Limit
In-Vitro	21.24	20.59*	21.89*
Ex-Vivo	30.86	29.49	32.03
24 Ex-Vivo	32.41	30.63	34.31
In-Vivo	56.00	54.70	57.60

*Note on fiducial limits-doses below the lower limit did not produce injury, and doses above the upper limit always produced injury

Table 2: Fixed Factor Correlation Relative to *In-vivo* Data Applied to Median Effective
Dose and Fiducial Limits of Tissue Response by Experimental Model

Model	Fixed Factor	ED$_{50}$ (J/cm^2)	95% Fiducial Limits	
			Lower Limit	Upper Limit
In-Vitro	2.64	56.07	54.36	57.79
Ex-Vivo	1.81	55.86	53.38	57.97
24 Ex-Vivo	1.73	56.07	52.99	59.36
In-Vivo	--	56.00	54.70	57.60
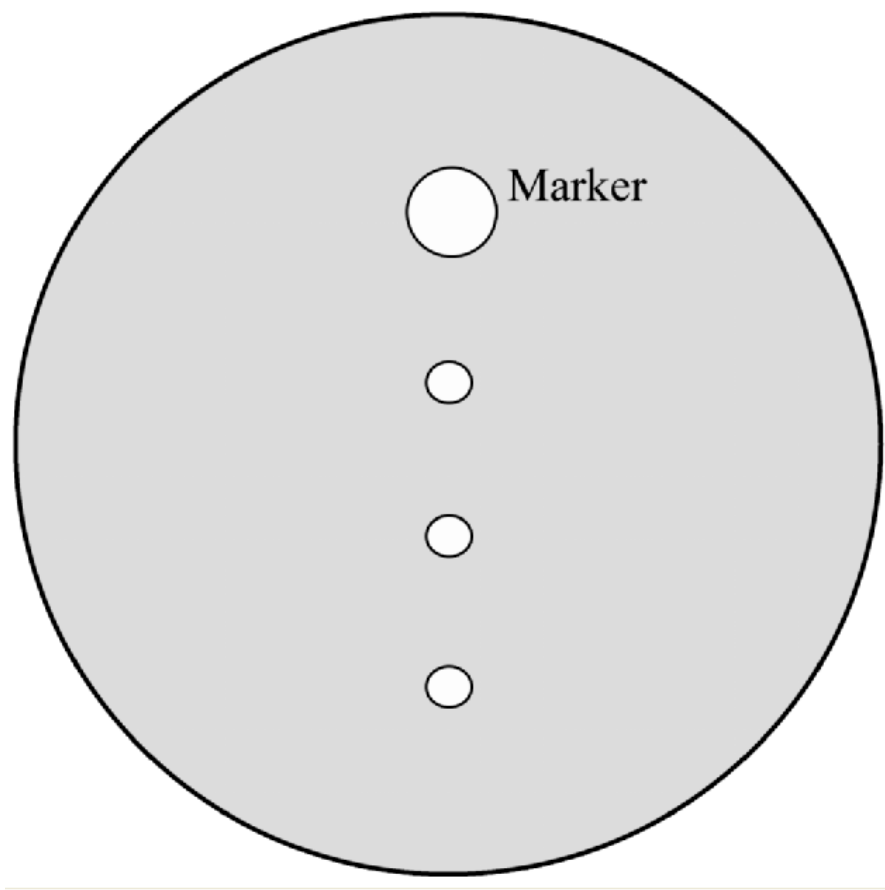
Figure 1: Cornea exposure diagram showing orientation marking lesion and experimental exposure sites.
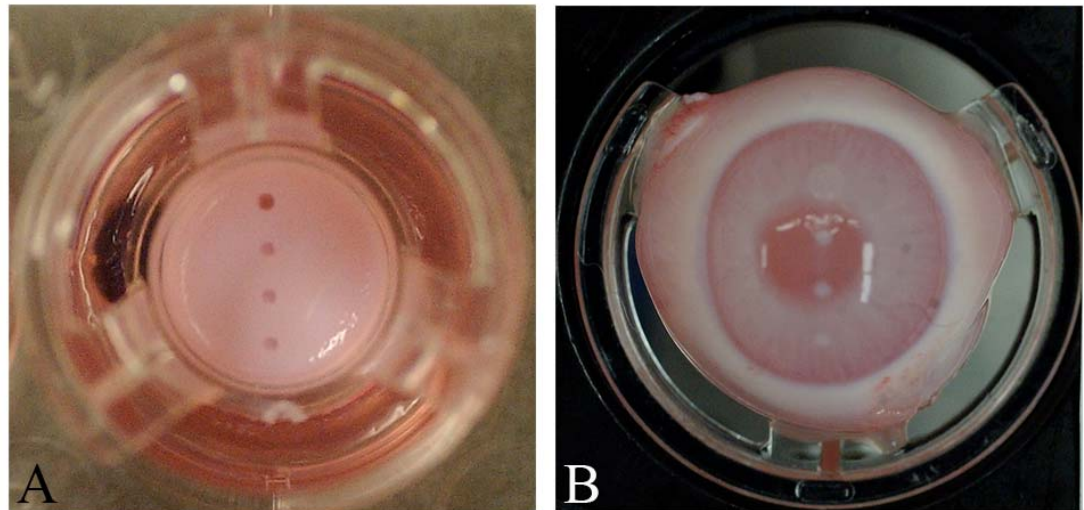
Figure 2: Digital photographs of corneal lesions immediately after laser exposures to *in-vitro* (left) and *ex-vivo* (right) corneal tissues. *In-vitro*: Marking lesion and experimental exposures appear as discrete, round holes in surface. *Ex-vivo*: Marking lesion and experimental exposures appear as discrete, raised, opaque areas on surface.
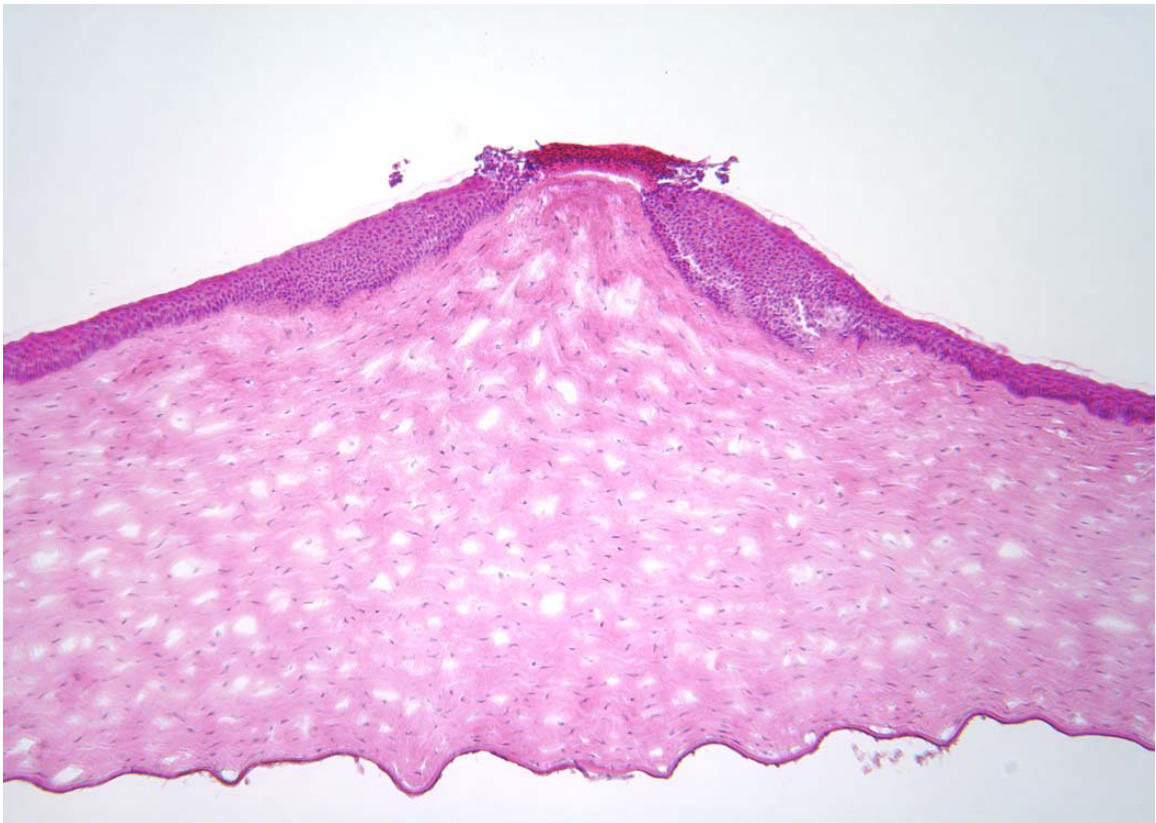
Figure 3: Representative image of damage to an *ex-vivo* rabbit cornea 24 hours after 1540 nm laser exposure at 37 J/cm^2. The epithelium within the beam path was markedly damaged. The stroma directly underlying the epithelial layer within the beam path showed an increased basophilia typical of thermal denaturation. The epithelial cells outside the beam path and adjacent to the damaged epithelium demonstrated a marked proliferation. Minimal cellular response was observed in the adjacent stroma. Original magnification = 63x
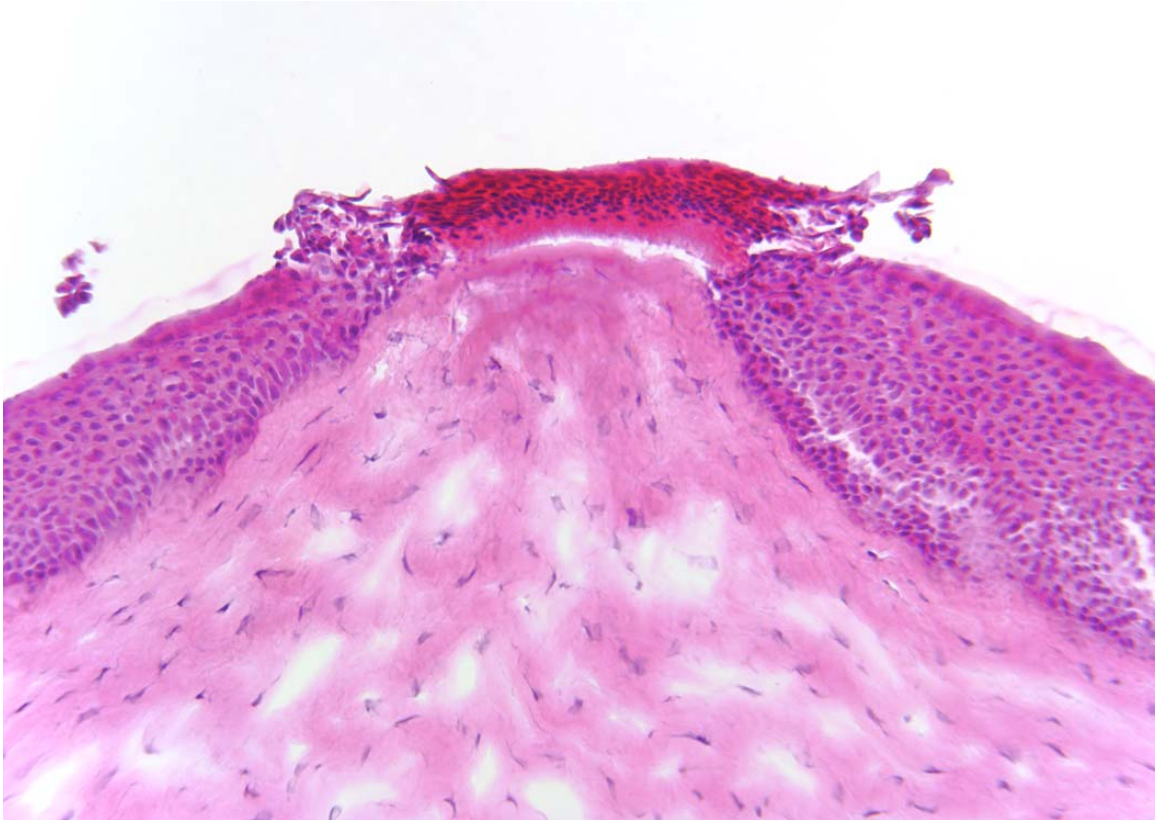
Figure 4: Higher magnification image of the *ex-vivo* rabbit cornea shown in Figure 3. The epithelial cells within the beam path demonstrated a distinct coagulative necrosis. There was a decreased number of stromal keratocytes within the area of increased stromal basophilia. The marked epithelial proliferation is primarily restricted to the cells of the *stratum basale* located outside the periphery of the beam path. Original magnification = 160x.
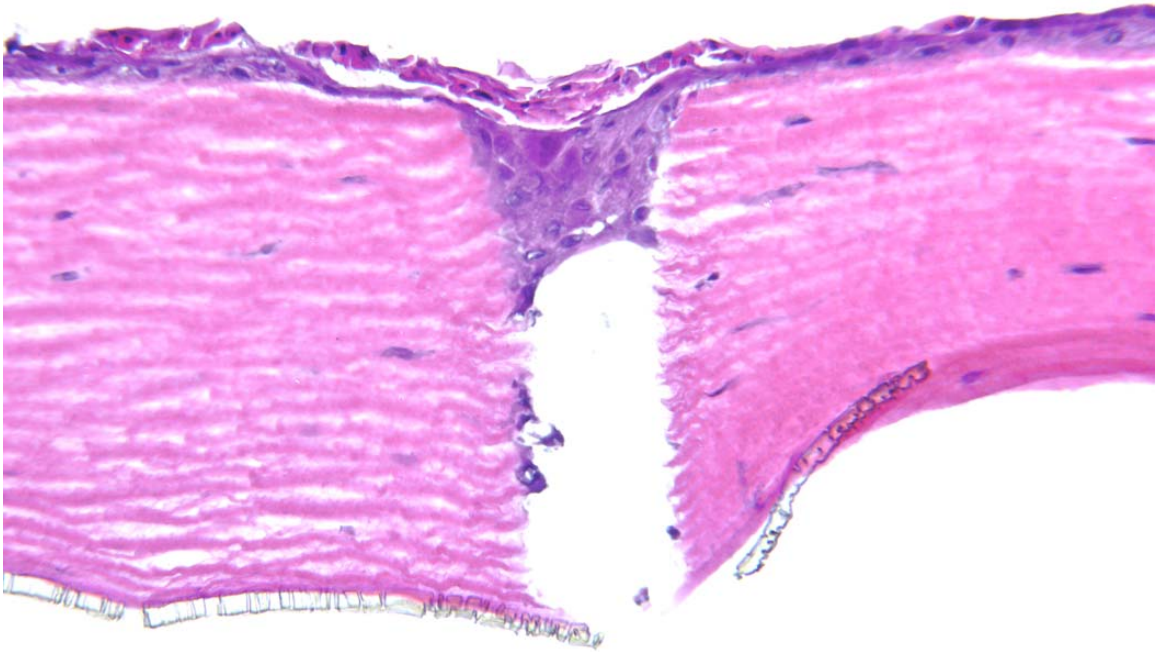
Figure 5: Representative image of damage to an *in-vitro* rabbit corneal model 24 hours after 1540 nm laser exposure at 28 J/cm^2. The most superficial layer of the epithelium within the beam path was markedly damaged. However, the underlying epithelial cells showed a proliferative response that was analogous to the *ex-vivo* rabbit cornea. The stromal matrix in the model tissue was affected more severely than the *ex-vivo* rabbit cornea with a distinct tissue ablation within the beam path. Original magnification = 160x.
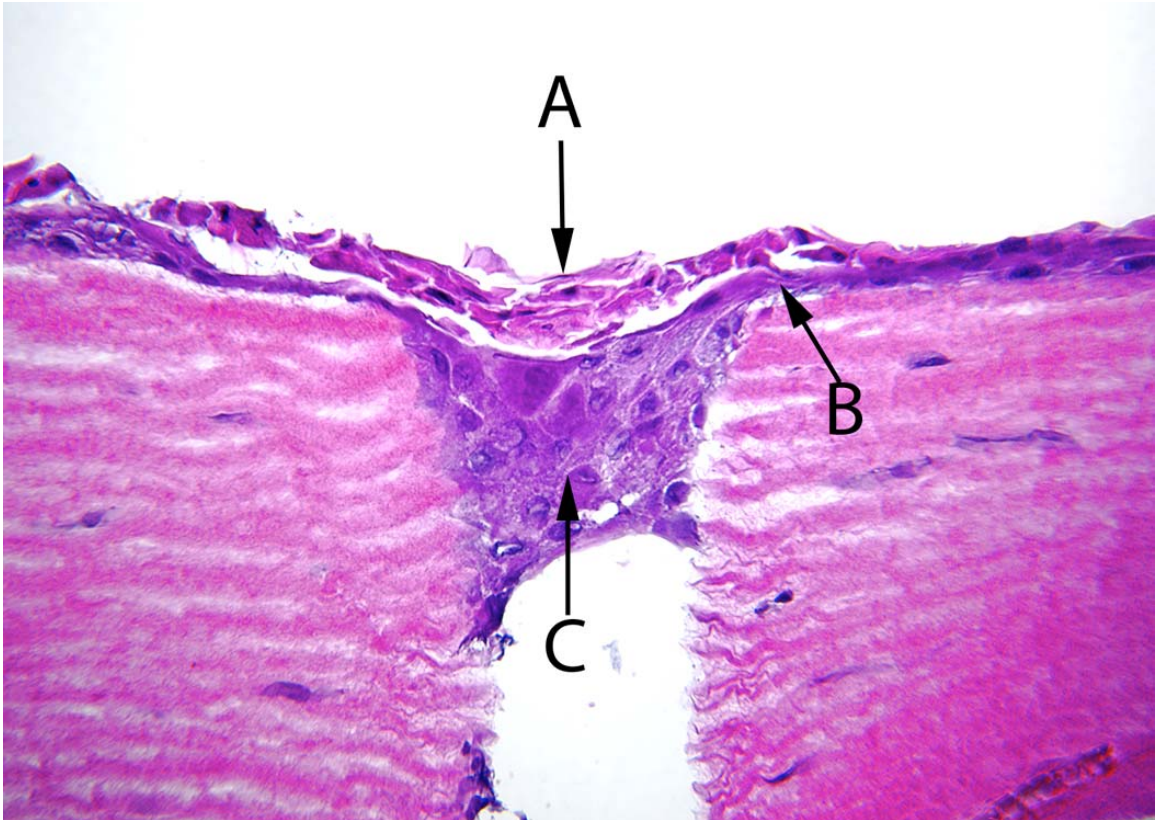
Figure 6: Higher magnification image of the *in-vitro* corneal model shown in Figure 5.

(A) Superficial layer of epithelial cells damaged by laser and not able to repair. (B)

Proliferating cells arising from the basal layer of the corneal epithelium. (C) Proliferating

cells seen filling the ablated tissue space produced by the laser energy. Original

magnification = 250x.

References Cited

1. Hamlin, S. J., A. D. Hays, C. W. Trussell, and V. King. 2004. Eye safe erbium glass microlaser. vol. 5332, p. 97-102. *In* R. Scheps and H. J. Hoffman, (ed.), Solid State Lasers XIII: Technology and Devices. Proceedings of the Society of Photo-Optical Instrumentation Engineers, The Society of Photo-Optical Instrumentation Engineers, San Jose, Calif.

2. Mayor, S. D., S. M. Spuler, and B. M. Morley. 2005. Scanning eye-safe depolarization lidar at 1.54 microns and potential usefulness in bioaerosol plume detection, vol. 5887, p. 137-148. *In* U. N. Singh (ed.), Lidar Remote Sensing for Environmental Monitoring VI. Proceedings of the Society of Photo-Optical Instrumentation Engineers, The Society of Photo-Optical Instrumentation Engineers, San Jose, Calif.

3. Sliney, D. H., J. Mellerio, V. Gabel, and K. Schulmeister. 2002. What is the meaning of threshold in laser injury experiments? Implications for human exposure limits. Health Phys. 82: 335-347.

4. Zander, E. and G. Weddell. 1951. Observations on the innervation of the cornea. J Anat. 85: 68.

5. Cogan, D. G. and V. E. Kinsey. 1942. The cornea V. Physioloci aspects. Arch Ophthal 28: 661.

6. Zaret, M. M., G. M. Breinin, H. Schmidt, H. Ripps, and I. M. Siegel. 1961. Ocular Lesions Produced by an Optical Maser (Laser). Science 134: 1525-1526.

7. Lund DJ, Landers MB, Bresnick GH, Powell JO, Chester JE, Carver C. Ocular hazards of the Q-switched erbium laser. Investigative Ophthalmol 9:463–470; 1970.

8. Avdeev et al. Experimental determination of maximum permissible exposure to laser of 1.54 u wavelength, Soviet J. Quantum Electronic 8:137-139 1978

9. Stuck BE, Lund DJ, Beatrice ES. Ocular effects of holmium (2.06 μm) and erbium (1.54 μm) laser radiation. Health Phys 40:835–846; 1981.

10. Clarke, T. F., T. E. Johnson, M. B. Burton, B. Ketzenberger and W. P. Roach. 2002. Corneal injury threshold in rabbits for the 1540 nm infrared laser. Aviat. Space Environ. Med. 73(8):787-790.

11. McCally RL, Bonney-Ray J, Bargeron CB. Corneal injury thresholds for exposures to 1.54-μm radiation—dependence on beam diameter. Health Phys 87:16–24; 2004.

12. Ham, W. T., and H. A. Mueller. 1991. Ocular effects of laser infrared radiation. J. Laser. Appl. 3(3):19-21.

13. Heisterkamp, A., T. Mamom, O. Kermani, W. Drommer, H. Welling, W. Ertmer and H. Lubatschowski. 2003. Intrastromal refractive surgery with ultrashort laser pulses: in vivo study on the rabbit eye. Graefes. Arch. Clin. Exp. Ophthalmol. 241(6):511-517.

14. Ketzenberger, B., T. E. Johnson, Y. A. Van Gessel, S. P. Wild, and W. P. Roach. 2002. Study of corneal lesions induced by 1,318-nm laser radiation pulses in Dutch belted rabbits (Oryctolagus cuniculus). Comp. Med. 52(6):513-517.

15. Miyamoto, T., S. Saika, A. Yamanaka, Y. Kawashima, Y. Suzuki, and Y. Ohnishi. 2003. Wound healing in rabbit corneas after photorefractive keratectomy and laser in situ keratomileusis. J. Cataract. Refract. Surg. 29(1):153-158.

16. Russell, W. M. S. and R. L. Burch. 1959. The Principles of Humane Experimental Technique. New York: Hypersion Books Inc.

17. Guaitani, A., L. De Francesco L, and S. Garattini. 1997. Reduced use of laboratory animals in research institute. Lancet. 349 (1064): 1557-1558.

18. Zurlo, J., D. Rudacille, and A. M. Goldberg. 1994. Animals and Alternatives to Animal Testing: History, Science and Ethics. Mary Ann Liebert, Inc. Larchmont, NY.

19. Siegman, A.E., Sasnett MW, Johnston JTF. 1991. Choice of clip levels for beam width measurements using knife-edge techniques. IEEE J. Quantum Electron. 27:1098-1104.

20. Walsh JT: Pulsed Laser Angioplasty: A Paradigm for Tissue Ablation. In Welch AJ, van Gemert MJC (eds) *Optical-Thermal Response of Laser Irradiated Tissue*. Plenum Press, NY, 1995.

21. Eurell, T. E., T. E. Johnson, and W. P. Roach. 2003. Histomorphometric and proteomic analysis of the acute corneal tissue response following in vitro exposure to 1540 nm laser light, vol. 4953, p. 113-116. *In* B. E. Stuck and M. Belkin (ed.), Laser and non-coherent light ocular effects: epidemiology, prevention and treatment. Proceedings of the Society of Photo-Optical Instrumentation Engineers, The Society of Photo-Optical Instrumentation Engineers, San Jose, Calif.

22. Bliss C.I. 1935. The Calculation of the Dosage Mortality Curve from Small Numbers. J. Pharmacol. 11:192-216.

23. Finney, D. J. 1971. Probit Analysis, 3rd ed. Cambridge University Press, Cambridge.

Chapter 5

Morphometric Comparison of the Acute Rabbit Corneal Response to 1540 nm Laser Light Following *Ex-vivo* Exposure to Millisecond and Nanosecond Pulse Widths

Morphometric Comparison of the Acute Rabbit Corneal Response to 1540 nm Laser Light Following *Ex-vivo* Exposure to Millisecond and Nanosecond Pulse Widths.

Nicole A. McPherson [1], Thomas E. Eurell [2*], Thomas E. Johnson [2]

Nicole A McPherson, MPH; Uniformed Services University of the Health Sciences, Bethesda, MD, 20814 Nmcpherson@usuhs.mil [1]

Thomas E. Eurell, DVM, PhD; Colorado State University, Fort Collins, CO, 80523 Thomas.Eurell@colostate.edu [2]

Thomas E Johnson, PhD; Colorado State University, Fort Collins, CO, 80523 Thomas.E.Johnson@colostate.edu [2]

Correspondence should be directed to Dr. Thomas E Johnson*

Colorado State University

1618 Campus Delivery
Fort Collins, CO 80523
Phone 970-491-0563
Fax 970-491-0623
Thomas.E.Johnson@colostate.edu

Abstract

The aim of the present study was to determine whether immunohistological analyses techniques visualizes areas of tissue damage differently when compared with histopathology. In addition, we intended to evaluate if the laser-tissue interaction of *ex-vivo* rabbit corneal tissue would vary in relation to the pulse width of a near-infrared (1540 nm) laser. We found the immunohistological analyses to give similar information in visualizing the lesion as the histopathology in determining the depth and width of the lesion for both the ns and ms pulse widths. Yet, the MMP-2 immunoreaction products area proportion to the lesion size was significantly different for the ns pulse width. This indicates the two analyses should be performed in concert to accurately describe the tissue damage post exposure.

1 Introduction

Lasers with wavelengths longer than approximately 1.4 μm are often called "eye-safe", because light in this wavelength range is strongly absorbed in the cornea and can not reach the retina to cause permanent damage to the eye. This absorption of the infrared lasers wavelengths is due to water being considered the principal chromophore. (Profio and Doiron 1987; van Gemert et al. 1989; Xu and Alfano 2005) This absorption characteristic is useful in refractive surgery of the eye because the cornea is approximately 80% water. (Heisterkamp et al. 2003; Kurtz et al. 1998; Sugar 2002) The specific wavelength of light also determines the depth it can penetrate into the tissue. This absorption of energy by the chromophore results in thermal energy. However, this also poses an increasing risk of accidental exposure and corneal damage as infrared lasers become more powerful and are used in more applications. (Clarke et al. 2002; Ketzenberger et al. 2002)

Objective evaluation of new laser-based refractive surgical methods and effective treatment of infrared laser damage requires accurate determination of post-exposure wound healing. (Daniels et al. 2003; Daniels and Khaw 2000; Esquenazi et al. 2005; Fini and Stramer 2005; Isnard et al. 2005; Kuo 2004; Miyamoto et al. 2003; Mulholland, Tuft, and Khaw 2005; Netto et al. 2005; Rossi et al. 2005) Studies with experimental animals are key elements in approaching accurate post-exposure wound healing. The rabbit is one of the most commonly reported experimental animals used to study laser-induced corneal wound healing.(Bargeron et al. 1989; Clarke et al. 2002; Freund et al. 1995; Heisterkamp

et al. 2003; Isnard et al. 2005; Jester et al. 2005; Ketzenberger et al. 2002; Kurtz et al. 1998; McCally et al. 1983)

Previous studies evaluating the effects of laser pulse width and pulse duration on ocular tissues have demonstrated that these laser parameters can have significant effects on laser-tissue interaction. (Brinkmann et al. 2000; Framme et al. 2004; Kurtz et al. 1998; Schuele et al. 2005; Vogel et al. Mechanisms of intraocular photodisruption with picosecond and nanosecond laser pulses 1994; Vogel et al. Intraocular photodisruption with picosecond and nanosecond laser pulses: Tissue effects in cornea, lens, and retina 1994) The theory of selective photothermolysis is based on targeting a chromosphere by laser energy absorption without thermal damage to surrounding tissue.(Carroll and Humphreys 2006) The pulse duration and spot size play important roles in determining where selective damage to tissue occurs without thermal damage occurring to the surrounding tissue.

The aim of the present study was to determine whether immunohistological analyses techniques visualizes areas of tissue damage differently when compared with the "gold standard," histopathology. In addition, we intended to evaluate if the laser-tissue interaction of *ex-vivo* rabbit corneal tissue would vary in relation to the pulse width of a near-infrared (1540 nm) laser.

2 Materials and Methods

2.1 *Ex-vivo rabbit corneas*

Rabbit eyeballs were obtained from animals undergoing terminal procedures not related to this study and without clinical signs of ocular disease. No live animals received laser exposures. All methods for the recovery of rabbit eyeballs following euthanasia

were approved by the University of Illinois Institutional Animal Care and Use Committee. Eyeballs were maintained at 4°C in Dulbecco's modified Eagle's medium (DMEM; Mediatech) supplemented with 10% Nuserum (BD Biosciences), 1% antibiotic/antimycotic (Sigma), and 0.05 % L-glutamine (Mediatech) and used for laser exposure within 24hr of enucleation.

2.2 *Laser Parameters and Tissue Exposure*

A Laser Sight Technologies, Inc (Winter Park, FL) Er:Glass laser emitting a single pulse at 1540 nm was used for all exposures. The laser could be configured for 0.8 ms pulse with a lens focusing to a 1.38E-4 ($1/e^2$) spot, or 400 ns pulse with a 1.64E-4cm^2 ($1/e^2$) spot. The spot size was determined using a knife-edge technique described by Siegman et al.(Siegman, Sasnett, and Johnston 1991)   Each exposure was measured using a beam splitter terminated with a Molectron EPM-2000 meter (Coherent) and a J25 energy detector (Coherent). A Thor Labs (PDA 255) Germanium photon detector connected to a Tektronix TDS 644B digitizing oscilloscope measured pulse duration. There were five exposures for each pulse width with fluence ranges of 54.99 to 60.41 J/cm^2 for the 400 ns pulse width and 54.26 to 57.87 J/cm^2 for the 0.8 ms pulse width.

2.3 *Tissue Processing and Analysis*

Immediately following laser exposure, control and experimental rabbit eyeballs were placed in petri dishes containing DMEM and incubated overnight at 37°C and 5% CO_2. Following overnight incubation, the corneas were surgically removed from the eyeballs using a circumferential incision at the limbal border, immersed in cryotome embedding medium (OCT compound, Sakura), quick frozen in liquid nitrogen and stored at -80°C until further processing.

Eight micron frozen sections of the corneas were made on sialinized glass slides (Fisher) and fixed in -20°C acetone for 10 min. All sections were then rehydrated in 10 mM phosphate buffered saline with a pH of 7.4 (PBS) for 15 minutes at room temperature. Following the PBS rehydration step, all sections were kept moist in a humidity chamber until further processing. Further processing was either staining for histopathology or immunohistochemistry.

Sections evaluated for histopathology were stained using Gill's #3 Hematoxylin for 30 seconds, rinsed in tap water for 5 minutes and counterstained using Eosin/Phloxine for 30 seconds. Stained sections were then dehydrated in a series of alcohols, dipped in xylene and mounted using Eukitt (Fisher).

Sections evaluated for immunohistochemistry were processed using CoverPlate Immunostaining Chambers (Shandon Scientific). Indirect immunostaining for matrix metalloproteinase-2 (MMP-2) was performed using a primary mouse monoclonal antibody (clone 42-5D11; Chemicon International) followed by a horseradish peroxidase (HRP) polymer secondary reagent (Zymed). Checkerboard titrations of primary mouse monoclonal antibody and the secondary HRP polymer reagent were used to establish appropriate dilutions of primary and secondary reagents. All incubation procedures were conducted following manufacturer's recommended procedures.

The immunohistochemistry reaction product (antibody-HRP complex) was detected using diaminobenzidine tetrahydrochloride (DAB; Sigma) following manufacturer's recommended procedures. The tissue was counterstained with Contrast Red (KPL). Controls for the immunostaining protocol included analysis of non-exposed corneal tissues and substituting normal mouse serum for the MMP-2 antibody. Digital

images of all stained sections were obtained using a Leitz Orthoplan microscope equipped with a SpotRT digital camera (Diagnostic Instruments). Quantitative histomorphometry was performed using Image Pro Plus analysis software (Media Cybernetics). Comparisons of histomorphometric data between mean values of treatment groups were conducted using Student's t-test when data normality and equal variance conditions were met. Mann-Whitney rank sum analyses were conducted when data did not pass normality or equal variance tests.

3 Results

3.1 *Histopathology*

Single pulse 1540 nm laser exposures had significant laser-tissue interaction with *ex-vivo* rabbit corneal tissues following the exposure and incubation conditions outlined above. Hematoxylin and eosin stained tissue sections revealed that the 0.8 ms laser exposures had more damaging histopathological effects than the 400 ns laser exposures (Fig. 1). Analysis of the morphometric data indicated that the differences in histopathology between the 0.8 ms and 400 ns laser exposures were significant (Table 2). The epithelium and stroma within the 0.8 ms beam path showed histological evidence of thermal denaturation and coagulative necrosis. Most of the epithelial layer has been ablated (Fig. 1, Frame A). Similar histopathological changes were seen following the 400 ns laser exposure, however, the general tissue response appeared less intense than those seen with the 0.8 ms laser (Fig. 1, Frame B).

3.2 *Morphometric Analyses of Hematoxylin and Eosin Stained Tissues*

Morphometric analyses of the laser induced corneal lesions demonstrated that in all cases the parameters measured for the 0.8 ms exposures were significantly greater ($P \leq$ 0.01) than the parameters measured 400 ns laser exposures (Table 1).

The mean maximum lesion diameter was measured at the surface of the lesion and reflects the spot size of the laser beam (1.38e-3 mm for the 0.8 ms exposures and 1.64E-4cm^2 for the 400 ns exposures).

The laser has a Gaussian beam profile. The Gaussian profile has an intensity peak at the center of the beam and then attenuates at the periphery of the beam. By knowing where the tissue was exposed by the laser and knowing the spot size of the beam, the tissue sections can be cut along this Gaussian beam profile to obtain the deepest portion of damage along the beam path.

3.3 *Immunohistological Analyses*

Single pulse 1540 nm laser exposures induced MMP-2 production detectable by immunohistological analyses in *ex-vivo* rabbit corneal tissues following the exposure and incubation conditions outlined above. Comparison of sections from laser treated and control rabbit corneas confirmed that specific MMP-2 immunoreaction products were restricted to the lesion area.

Although smaller in absolute values, the maximum lesion diameter and maximum lesion depth determined using the MMP-2 immunoreaction products (Table 2) were similar to the analogous histopathological data (Table 1). The general pattern of MMP-2 immunoreaction products for the ms exposures occurred at the margins of the lesion and represented a relatively small portion (approximately 36%) of the total lesion area.

However, in all cases of ns laser exposures, the MMP-2 immunoreaction products appeared to fill most of the lesion area.

4   Discussion

With the use of laser-based therapies for dermatology and refractive surgeries examining the effects on wound repair should prove to be clinically important. This study documents the response of the corneal tissue to the 1540 nm laser using two different pulse widths and two separate spot sizes then compares standard histology to immunohistological analyses to determine if the characterization of the injury and healing is different.

As expected the histology shows that the 0.8 ms pulse duration has a greater lesion diameter, depth and total area than the 400 ns pulse duration. But an unexpected finding was that proportionally the immunohistology total area was greater for the 400 ns pulse duration than the 0.8 ms pulse duration. This difference indicates a differential response in the MMP-2 expression and ultimately wound repair of the two lesion types. MMP expression levels have been shown to be greater in wounds showing evidence of rapid healing versus standard burn injuries that exhibit slow healing responses.(Schaffer et al. 1997)

Perhaps this difference is due to the pulse duration of the lesions, since the pulse duration of the laser needs to be shorter than the thermal relaxation time of the target chromophore in order to prevent the spread of thermal energy beyond the target chromophore. The 1540 nm lasers target chromophore is water. If the pulse duration is greater than the thermal relaxation time then non-specific thermal damage may occur due

to heat diffusion.(Carroll and Humphreys 2006) The 0.8 ms pulse duration may act more closely to standard burn injury than the 400 ns pulse duration and therefore expressed less MMP-2 in the wound.

The MMP-2 expressed in both pulse duration lesions were overall approximately 80 % of the histology's depth and diameter. The proportion could be utilized to predict the histopathology of the lesions. (Table 3)

In conclusion, both pulse durations showed similarity in their morphological and histological analyses, but differed in there MMP-2 proportional expression. This MMP-2 difference shows that both histology and immunohistology analyses should be used in concert to characterize the wound and may help lead to more useful wound therapies in the future.

Acknowledgements

Table 1 Mean morphometric values[a] obtained from H&E stained corneal tissue.

Pulse Width	Mean Maximum Lesion Diameter[b]	Mean Maximum Lesion Depth[b]	Mean Total Area Of Lesion[c]
0.8 MS	552.7 ± 5.9	701.3 ± 16.7	133, 881.0 ± 665.7
400 NS	163.9 ± 2.1	415.5 ± 2.9	28, 566.6 ± 176.7

[a] all values are in microns ± 1 SD
[b] each mean was calculated from sample size n=5 that was measured twice
[c] each mean was calculated from a sample size n=5

Table 2 Mean morphometric values[a] of immunoreaction DAB products obtained from corneal tissues incubated with antibody against MMP-2.

Pulse Width	Mean Maximum Lesion Diameter[b]	Mean Maximum Lesion Depth[b]	Mean Total Area Of Lesion[c]
0.8 MS	468.8 ± 7.2	581.1 ± 6.7	48,666.4 ± 1, 225.4
400 NS	145.7 ± 3.0	334.9 ± 2.6	28, 867.4 ± 831.3

[a] all values are in microns ± 1 SD
[b] each mean was calculated from sample size n=5 that was measured twice
[c] each mean was calculated from a sample size n=5

Table 3 Proportional values of mean immunoreaction DAB products to mean morphometric values

Pulse Width	Mean Maximum Lesion Diameter[b]	Mean Maximum Lesion Depth[b]	Mean Total Area Of Lesion[c]
0.8 MS	0.85	0.83	0.36
400 NS	0.89	0.81	1.01

[b] each mean was calculated from sample size n=5 that was measured twice
[c] each mean was calculated from a sample size n=5
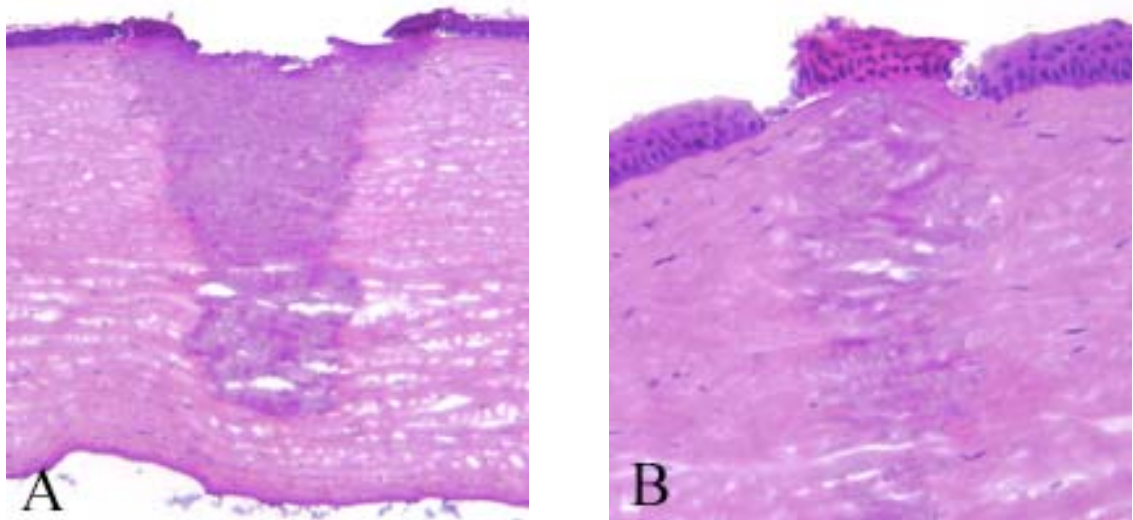
Fig. 1 Histopathology of representative sections from rabbit corneas following 0.8 ms and 400 ns laser exposure. **A.** Cornea exposed to a single pulse of 0.8 ms 1540 nm laser light with a 1.38E-4 cm^2 spot size and an energy density range of 54.26 to 57.87 J/cm^2 J/cm^2 at $1/e^2$. Original magnification = 63x. **B.** Cornea exposed to a single pulse of 400 ns 1540 nm laser light with a 1.64E-4 cm^2 spot size and an energy density range of 54.99 to 60.41 J/cm^2 at $1/e^2$. Original magnification = 160x.
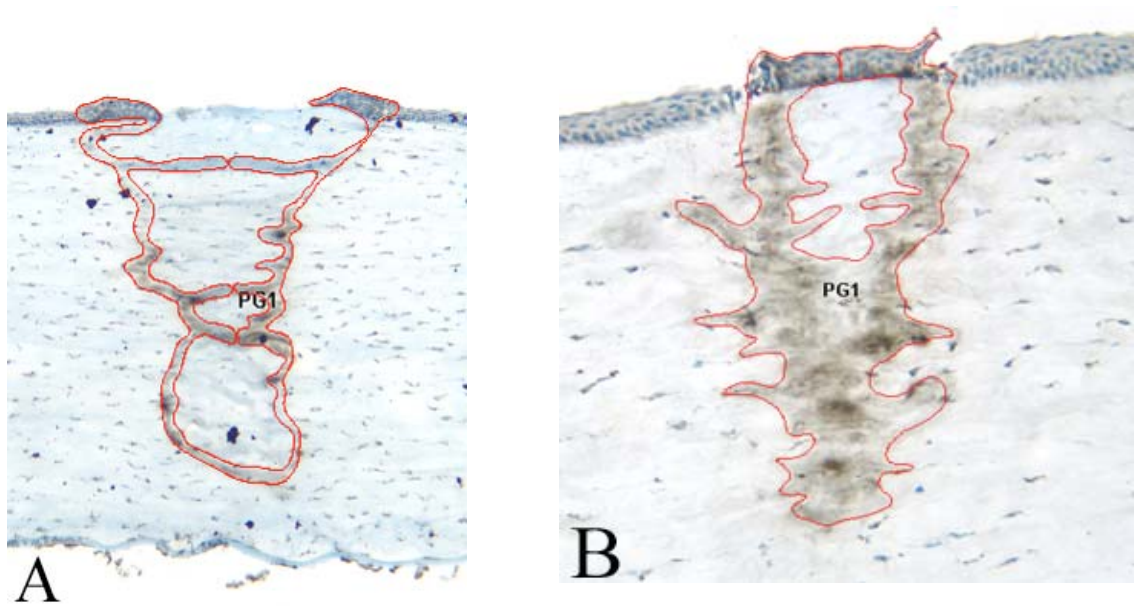
Fig. 2 Histomorphometry of representative MMP-2 immunoreaction products in rabbit corneas following 0.8 ms and 400 ns laser exposure. **A**. Cornea exposed to single pulse 0.8 ms 1540 nm laser light with 1.38E-4 cm^2 spot size and an energy density range of 54.26 to 57.87 J/cm^2 at $1/e^2$. PG1=area of DAB immunoreaction product. Original magnification = 63x. **B.** Cornea exposed to single pulse 400 ns 1540 nm laser light with 1.64E-4 cm^2 spot size and an energy density range of 54.99 to 60.41 J/cm^2 at $1/e^2$. Original magnification = 160x.

References Cited

Bargeron CB, Deters OJ, Farrell RA, McCally RL. Epithelial damage in rabbit corneas exposed to CO2 laser radiation. Health Phys 56: 85-95; 1989.

Brinkmann R, Huttmann G, Rogener J, Roider J, Birngruber R, Lin CP. Origin of retinal pigment epithelium cell damage by pulsed laser irradiance in the nanosecond to microsecond time regimen. Lasers Surg Med 27: 451-64; 2000.

Carroll L, Humphreys TR. LASER-tissue interactions. Clinics in Dermatology 24: 2-7; 2006.

Clarke TF, Johnson TE, Burton MB, Ketzenberger B, Roach WP. Corneal injury threshold in rabbits for the 1540 nm infrared laser. Aviat Space Environ Med 73: 787-90; 2002.

Daniels JT, Geerling G, Alexander RA, Murphy G, Khaw PT, Saarialho-Kere U. Temporal and spatial expression of matrix metalloproteinases during wound healing of human corneal tissue. Exp Eye Res 77: 653-64; 2003.

Daniels JT, Khaw PT. Temporal stimulation of corneal fibroblast wound healing activity by differentiating epithelium in vitro. Invest Ophthalmol Vis Sci 41: 3754-62; 2000.

Esquenazi S, He J, Bazan NG, Bazan HE. Comparison of corneal wound-healing response in photorefractive keratectomy and laser-assisted subepithelial keratectomy. J Cataract Refract Surg 31: 1632-9; 2005.

Fini ME, Stramer BM. How the cornea heals: cornea-specific repair mechanisms affecting surgical outcomes. Cornea 24: S2-S11; 2005.

Framme C, Schuele G, Roider J, Birngruber R, Brinkmann R. Influence of pulse duration and pulse number in selective RPE laser treatment. Lasers Surg Med 34: 206-15; 2004.

Freund DE, McCally RL, Farrell RA, Cristol SM, L'Hernault NL, Edelhauser HF. Ultrastructure in anterior and posterior stroma of perfused human and rabbit corneas. Relation to transparency. Invest Ophthalmol Vis Sci 36: 1508-23; 1995.

Heisterkamp A, Mamom T, Kermani O, Drommer W, Welling H, Ertmer W, Lubatschowski H. Intrastromal refractive surgery with ultrashort laser pulses: in vivo study on the rabbit eye. Graefes Arch Clin Exp Ophthalmol 241: 511-7; 2003.

Isnard N, Bourles-Dagonet F, Robert L, Renard G. Studies on corneal wound healing. Effect of fucose on iodine vapor-burnt rabbit corneas. Ophthalmologica 219: 324-33; 2005.

Jester JV, Budge A, Fisher S, Huang J. Corneal keratocytes: phenotypic and species differences in abundant protein expression and in vitro light-scattering. Invest Ophthalmol Vis Sci 46: 2369-78; 2005.

Ketzenberger B, Johnson TE, Van Gessel YA, Wild SP, Roach WP. Study of corneal lesions induced by 1,318-nm laser radiation pulses in Dutch belted rabbits (Oryctolagus cuniculus). Comp Med 52: 513-7; 2002.

Kuo IC. Corneal wound healing. Curr Opin Ophthalmol 15: 311-5; 2004.

Kurtz RM, Horvath C, Liu HH, Krueger RR, Juhasz T. Lamellar refractive surgery with scanned intrastromal picosecond and femtosecond laser pulses in animal eyes. J Refract Surg 14: 541-8; 1998.

McCally RL, Bargeron CB, Green WR, Farrell RA. Stromal damage in rabbit corneas exposed to CO2 laser radiation. Exp Eye Res 37: 543-50; 1983.

Miyamoto T, Saika S, Yamanaka A, Kawashima Y, Suzuki Y, Ohnishi Y. Wound healing in rabbit corneas after photorefractive keratectomy and laser in situ keratomileusis. J Cataract Refract Surg 29: 153-8; 2003.

Mulholland B, Tuft SJ, Khaw PT. Matrix metalloproteinase distribution during early corneal wound healing. Eye 19: 584-8; 2005.

Netto MV, Mohan RR, Ambrosio R, Jr., Hutcheon AE, Zieske JD, Wilson SE. Wound healing in the cornea: a review of refractive surgery complications and new prospects for therapy. Cornea 24: 509-22; 2005.

Profio AE, Doiron DR. Transport of light in tissue in photodynamic therapy. Photochem Photobiol 46: 591-9; 1987.

Rossi F, Pini R, Menabuoni L, Mencucci R, Menchini U, Ambrosini S, Vannelli G. Experimental study on the healing process following laser welding of the cornea. J Biomed Opt 10: 024004; 2005.

Schaffer C, Reinisch L, Polis S, Stricklin G, Nanney L. Comparisons of wound healing among excisional, laser created, and standard thermal burns in porcine wounds of equal depth. Wound repair and regeneration 5: 52-61; 1997.

Schuele G, Rumohr M, Huettmann G, Brinkmann R. RPE damage thresholds and mechanisms for laser exposure in the microsecond-to-millisecond time regimen. Invest Ophthalmol Vis Sci 46: 714-9; 2005.

Siegman A, Sasnett M, Johnston J. Choice of clip levels for beam width measurements using knife-edge techniques. IEEE J Quantum Electron 27: 1098–1104; 1991.

Sugar A. Ultrafast (femtosecond) laser refractive surgery. Curr Opin Ophthalmol 13: 246-9; 2002.

van Gemert MJ, Jacques SL, Sterenborg HJ, Star WM. Skin optics. IEEE Trans Biomed Eng 36: 1146-54; 1989.

Vogel A, Busch S, Jungnickel K, Birngruber R. Mechanisms of intraocular photodisruption with picosecond and nanosecond laser pulses. Lasers Surg Med 15: 32-43; 1994.

Vogel A, Capon MR, Asiyo-Vogel MN, Birngruber R. Intraocular photodisruption with picosecond and nanosecond laser pulses: tissue effects in cornea, lens, and retina. Invest Ophthalmol Vis Sci 35: 3032-44; 1994.

Xu M, Alfano RR. Fractal mechanisms of light scattering in biological tissue and cells. Opt Lett 30: 3051-3; 2005.

Chapter 6

Characterization of corneal temperature change in an *in-vivo* (rabbit) model from
repeated exposures from a 1.54 micron laser

Characterization of corneal temperature change in an *in-vivo* (rabbit) model from repeated exposures from a 1.54 micron laser

Nicole A McPherson, MPH; Uniformed Services University of the Health Sciences, Bethesda, MD, 20814 Nmcpherson@usuhs.mil [1]

Thomas E. Eurell, DVM, PhD; Colorado State University, Fort Collins, CO, 80523 Thomas.Eurell@colostate.edu [2]

Barbara L. O'Kane, PhD, US Army RDECOM CERED NVESD, 10221 Burbeck Road, Fort Belvoir, VA 22060-5806, Barbara.okane@us.army.mil

Thomas E Johnson, PhD; Colorado State University, Fort Collins, CO, 80523 Thomas.E.Johnson@colostate.edu [2]

Correspondence should be directed to Dr. Thomas E Johnson*

Colorado State University

1618 Campus Delivery
Fort Collins, CO 80523
Phone 970-491-0563
Fax 970-491-0623
Thomas.E.Johnson@colostate.edu

Abstract

In order to reduce the number of animals utilized in laser injury studies multiple exposures across the eye are utilized as the data points. In the mid-infrared spectrum the mechanism for injury is largely thermal. This study was conducted to characterize the thermal effects after a laser exposure. Then this information was used to determine if there would be a rise in temperature in the eye after three successive exposures across the eye using a 1540 nm laser with 0.8 ms pulse duration in the *in-vivo* (rabbit) model. The fluence range for the 48 exposures was 68.78 J/cm^2 to 81.83 J/cm^2. We found the mean change in corneal temperature of the eye to be 28.41 (18.88 to 42.62) ^{o}C during the peak exposure. Five seconds post exposure the cornea's mean change in temperature was1.08 ^{o}C higher than before the exposure, which was significant at α=0.05 level. Histology showed a full thickness corneal injury (436.5 microns) from the laser exposures. The histology also showed the endothelial cells proliferating in stratified layers across the width of the laser exposure. Further research into the thermal characteristic and heat dissipation of the cornea are required to determine if the rise in temperature after each exposure requires modification to the current maximum permissible exposure limits. Investigation into the mechanisim triggering the endothelial cellular response is also warranted in hopes of finding a way to replicate this in humans.

Introduction

This study was initiated to investigate the thermal characteristics of an ocular injury resulting from a 1.54 micron laser. This is a part of a larger project to examine the effects of the 1.54 micron laser on the eye and evaluate potential therapies to heal such injuries. Currently the American National Standards Institute "Safe Use of Lasers" standard bases the maximum permissible exposure (MPE) standards off of median effective dose to cause an injury (ED_{50}). The ED_{50} thresholds utilized are from various laboratories and there is a certain variability among the data due to differences in standardization, calibration and biological variability in response among tissues.

One of the differences between the laboratories is how many laser exposures are performed per eye. Some laboratories use a single exposure per eye as a data point. Some laboratories use multiple exposures across an eye and use each exposure as a separate data point; this allows the researcher to use fewer animals in determining the ED_{50}. When looking at multiple exposures MPE, the standards are based on multiple exposures to the same exposure site, not separate exposures across the eye.

A previous study in the infrared by McCally et al examined the effect of multiple pulses of IR (2.02 micron) lasers on the cornea. They examined a single pulse to each eye and also 1, 10, 20 and 100 Hz pulse repetition rates. Pulse rates slower than one per second (1 Hz) do not appear to have been investigated. They found that damage was underestimated for small numbers of pulses. Further, corneal temperature was only calculated in the study, and not measured (McCally, Farrell, and Bargeron 1992).

Ex-vivo cornea temperature rise has been measured in a previous study(Bargeron, McCally, and Farrell 1981) and the temperature rise in an *in-vivo* corneal study with exposure from a carbon-dioxide laser is reported in the literature.(Mikesell 1978) These studies appear to have used only one exposure per eye, whereas this study used three separate exposures to the eye from a 1.54 micron laser. Multiple exposures across the eye are currently viewed as independent data points, but if the temperature of the cornea remains elevated between exposures then the data cannot be evaluated independently and it may impact the MPE limits.

Since only thermal effects occur in the far infrared spectrum (1.4 microns to 1 mm) the purpose of this study is to characterize the thermal effects from three separate exposures per cornea from a 1.54 micron laser and tries to determine if there is a change in the baseline temperature of the cornea after each exposure.

Materials and Methods

Laser

An Erbium-Glass laser was utilized for all exposures (Laser Sight Technologies, Inc Winter Park, FL). The laser produced single 0.8 ms pulses at 1540 nm. An LA 1708 lens using BK-7 glass (Newport, Ca) with a focal length of 50 mm was used. The *in-vivo* corneas were positioned at a distance of 54 mm from the lens. The spot size was

determined using a knife-edge technique described by Siegman et al.(Siegman AE 1991) Energy was measured with a Molectron EPM-2000 meter (Coherent, City, CA) and a J25 energy detector (Coherent, City, CA). Pulse duration was measured with a Germanium photon detector (PDA 255) from Thor Labs (Newton, NJ) connected to a Tektronix TDS 644B digitizing oscilloscope (Beaverton, OR). The beam had a Gaussian

profile and was approximately 2.18E-03 cm^2 in area. Exposures ranged from 68.78J/cm^2 to 81.83 J/cm^2 with an average fluence of 76.93 J/cm^2 and S.D. of 3.61 J/cm^2.

Imaging System

The imaging system utilized to record the radiometric temperature from the surface of the cornea was a thermal imaging system model SC2000 (FLIR) Systems, Boston, MA). The SC2000 has an internally calibrated microbolometer (320X240 pixels) with a built in 24-degree lens. The camera was positioned on a tripod mounted on the laser table at approximately 12 inches from the corneal exposure location.

Image Analysis

The FLIR system's ThermaCam Researcher 2002 was used to analyze the thermal imagery. Analysis was conducted by placing a spot on the center of the hot spot created by the laser on the cornea. This spot was labeled spot 1. The emissivity and distance settings were entered into the program for accurate analysis.

A reference temperature, spot 2, was utilized to reduce the effect of the change in pixel due to non-uniformity correction (NUC) occurring in the imagery collection timeframe for any particular exposure. The reference temperature location was determined by finding a location on the cornea that was similar in temperature to exposure location before the exposure occurred. The difference between the reference temperature and the exposure temperature prior to the exposure or the NUC was then subtracted from the difference of the reference temperature and the exposure temperature during the exposure sequence. This difference becomes the amount of rise in temperature due to the exposure. The reference temperature always comes from the location of Spot 2 in the image and the exposure temperature always comes from Spot 1 in the image. (See

figures 1 and 2) During thermal imaging the date and time of the exposure sequence was also recorded.

Statistical Analysis

SPSS was utilized to calculate the descriptive statistics of mean temperature rise, mean change in temperature between exposures, and the time between exposures. Pearson's Correlation Coefficient for time between exposure sets and the change in temperature between baselines of the exposure sets was also examined. Paired t-tests were performed on the data in SPSS with $\alpha = 0.05$.

Animal Exposures

The procedures were performed under an animal use protocol approved by the Institutional Animal Care and Use Committee (IACUC) at Uniformed Services University of Health Sciences (USUHS). USUHS is fully accredited by the American Association for Accreditation of Laboratory Animal Care (AAALAC), International. Eight male Dutch-belted rabbits were obtained from Covance Inc., Princeton, NJ with ages that ranged from 1-2 years old and weights from 2-3 kg. All animals were housed in accordance with the *Guide for the Care and Use of Laboratory Animals*[6] and participated in an environmental enrichment program at USUHS.

Rabbits were maintained under anesthesia throughout exposure. Buprenorphine (0.05 mg/kg, IM, Reckitt & Colman Pharmaceuticals, Inc., Richmond, VA) was administered intramuscularly for analgesia prior to recovery from anesthesia and at 8-hour intervals post procedure.

Corneal laser exposures involved placing rabbits on a platform in sternal recumbancy. An ocular speculum was used to keep the rabbit's eye open during

exposures. Proper positioning was determined with the use of a co-linear HeNe alignment beam. Three laser exposures per cornea were conducted in a horizontal linear fashion moving from medial to lateral on both eyes.

Saline drops were not administered between exposures. The tear film layer of the rabbit is reported at 7μ thick(Peppers et al. 1969) and the rabbit is able to maintain a constant thickness of tear film layer without blinking over a long amount of time.(Mishima 1965) Saline was used as a treatment option in the overall study and might have become a confounder for the treatment results.

Following the study, rabbits were euthanized using Sodium Pentobarbital 390 mg/ml (1 ml/rabbit) administered by intracardiac injection in accordance with the American Veterinary Medical Association 2000 Panel on Euthanasia[7] and the approved protocol.

Preparation of Corneal Tissues for Histological Evaluation

The eyes were enucleated and gross pictures of the globes were taken with a Nikon D100 Camera and a macroscopic lens. A 27 gauge needle was used to perforate the globe at the 12 o'clock position and tissue dye was used to highlight the perforation. The corneas were then dissected from the globes and embedded in cryotome embedding medium (OCT, Sakura FineTech, Torrance, CA) in a 5 ml disposable beaker. The lesions were oriented with the marking perforation at the 12 o'clock position and subsequent lesions along the centerline. The corneas were then placed in a freezing bath of hexane surrounded by liquid nitrogen. The frozen 5 mL disposable beaker was removed, covered with aluminum foil, placed into a labeled cryostorage bag and stored at -80°C until processed for histology.

Sections of the corneal tissue were made using a motorized cryomicrotome (Bright Instruments, Huntingdon, England). The tissues were trimmed in the cryomicrotome until the highlighted marking lesion was revealed. The micrometer on the cryomicrotome was then set and the tissues trimmed to reveal the exposure sites that were approximatley 2.5 mm apart. The marking lesion and the approximate spacing of the exposure sites allowed sectioning of the lesions with micrometer precision and accurately resolved the inside, middle and outside edges of the laser lesion.

Corneal sections were stained using Gill's #3 Hematoxylin for 30 seconds, rinsed in tap water for 5 minutes and counterstained using Eosin/Phloxine for 30 seconds. Stained corneal sections were then dehydrated in a series of alcohols, dipped in xylene and mounted using Eukitt (Electron Microscopy Services, Hatfield, PA). Images were captured using a Leitz Orthoplan microscope equipped with a SpotRT digital camera (Diagnostic Instruments, Sterling Heights, MI). Criteria used to evaluate the tissue responses to the 1.54 micron laser exposure included alterations in the epithelial parameters (e.g., area of hyaline coagulative change vs. area of granular coagulative change), stromal parameters (e.g., area of coagulative necrosis, number and distribution of keratocytes) and depth of damage.

Results

The fluence range for the 48 exposures was 68.78 J/cm^2 to 81.83 J/cm^2. The laser was set to produce exposures at approximately the ED$_{75}$. The ED$_{75}$ was chosen to ensure that a visible injury would be produced from each exposure. Each exposure was graded by two independent graders for the presence or absence of a visible lesion 1 minute and

24 hours after exposure. All exposures produced a visible lesion. The gross appearance of the lesions appeared as raised round white opaque area at the exposure site.

Miksell reported the normal mean corneal temperature from 172 Dutch belted rabbits without anesthesia as 34.67 ºC.(Mikesell 1978) In this study we found the mean baseline temperature 1 to be 35.33 ºC with a SE of 0.20 for Dutch belted rabbits under anesthesia. Baseline temperature 1 is defined as the temperature of the rabbit cornea under anesthesia prior to the first laser exposure, while baseline temperature 2 and baseline temperature 3 are the temperature of the eye prior to the corresponding exposure 2 and exposure 3. (See table 1)

Data was analyzed using a paired t-test to determine if there was a difference in the corneal temperature after successive exposures from the baseline temperature. In all cases, five seconds after exposure to the laser pulse the mean corneal temperature of the cornea was significantly different than the corresponding baseline exposure. (See table 4) It was also found that the temperature of the cornea from baseline temperature 1 to baseline temperature 2 did not change significantly. There was however a significant difference from baseline temperature 1 to baseline temperature 3 and baseline temperature 2 to baseline temperature 3 at α=0.05 level for the paired t-test. (See table 4) When comparing baseline temperature 1 to five seconds after exposure 3 there was not a significant difference. However, only two measurements were made, and this is considered insufficient to draw any conclusions.

The SC2000 thermal imaging system recorded the date time of the exposure sequence. This information was used to determine the time between exposures. (See table 2) The mean time between exposure set 1 and 2 and 2 and 3 were compared and were

not significantly different at α=0.05 level for the paired t-test. (See table 4) The time

between exposures was analyzed to determine if there was a correlation between the time

between exposures and the difference between the mean baseline temperatures for the

exposures. No correlation was found. (See table 3)

Histology

There is a discrete, full thickness lesion (436.5 microns deep) in the cornea

produced by the laser exposure. (See Figure 3 and Table 6) The overlying epithelial layer

is reduced in thickness with an apparent loss of stratification. Individual epithelial cells

show histological evidence of karyolysis. The underlying stromal tissue within the beam

path shows the basophilia characteristic of thermal denaturation. There is a marked

reduction in the number of stromal fibroblasts within the beam path. On the left and right

margins of the lesion there are zones of fibroblast proliferation that run parallel to the

beam path. (see figure 4)There is a noticeable proliferation and stratification of

endothelial cells within the beam path compared to normal areas of the cornea. (see

figure 5 and 6)

Discussion

Clarke et al reports the ED_{50} for the 1540 nm laser with a 0.8 ms pulse width as

56 J/cm^2. The ED_{75} was estimated from this data and utilized in this study. In Clarke's

study multiple exposure points across the cornea were used to determine the ED_{50}.(Clarke

et al. 2002)

When the peak temperature from exposure one to the peak temperature of

exposure three are compared, no significant difference between the mean temperatures of

the groups was found. This indicates that the peak temperatures from laser exposure in

each eye were not different and should not have impacted the baseline temperatures between baseline 1 and baseline 3 and between baseline 2 and baseline 3. (See table 4)

When the time between exposure sets are compared, there are no significant differences, again indicating no significant difference in the amount of time between exposures. The Pearson's correlation coefficient shows no correlation of the difference in time with the difference in temperature between sets. These results indicate the possibility that successive laser exposure to the cornea contributed to the change in temperature between the baseline temperature sets, even when there is greater than 11 seconds between exposures.

The threshold for thermal damage to the cornea has been documented by Peppers et al at 35 $^{\circ}$C above the baseline temperature of the cornea for the CO_2 laser. The critical temperature for thermal denaturizing of protein occurs at about 63 $^{\circ}$C for hemoglobin and at about 61 $^{\circ}$C for egg albumen for heating times of many seconds.(Peppers et al. 1969) This work demonstrates that the mean corneal temperature change of 28.41°C, ranging from 18.88 to 42.62 $^{\circ}$C, still caused damage to the cornea without reaching the critical temperature of 67 $^{\circ}$C when done at a 0.8 ms pulse with a 1540 nm laser.

In calculating the temperature increase expected from the exposure sets Buettner's equation for Δ T was utilized:

$$\Delta T = \frac{2\Phi_0 \sqrt{t}}{\sqrt{\pi \rho c_v}} \qquad (1)$$

Where ρ, and c_v are the corneal density (1.062 g/cm^3), and specific heat (3.83 J/g $^{\circ}$C) of the cornea and Φ_0 is the incident radiant exposure (J/cm^2) and t is the pulse duration in seconds. (Buettner 1951; Rossi, Pini, and Menabuoni 2007)

The mean calculated temperature rise for our data was 16.33 $^{\circ}$ C (14.6 to 17.37 $^{\circ}$ C). The disparity between the calculated and measured may be due to the beam profile. The laser has a Gaussian beam profile. The Gaussian profile has an intensity peak at the center of the beam and then attenuates at the periphery of the beam. The beam's spot size and the short pulse duration may have contributed to our measured temperature rise being higher than the calculated temperature rise. There may be a combination of models needed to explain the temperature response that occurs to the cornea at this pulse duration. The mechanism of thermal damage is not well understood in the shorter pulse durations.

As seen in the histology of the laser exposures, the exposure was absorbed through the depth of the cornea. It is unknown if the exposure went past the cornea as histology was not performed on the entire globe. It is unusual that the endothelial cells are stratified and proliferating. In both *ex-vivo* and *in-vitro* models the epithelial layers were shown to be proliferating and not the endothelial layer. The rabbit, unlike the human cornea, can regenerate endothelium cells *in-vivo*. Endothelium cells are regenerated in a monolayer. The histology images depict a stratified layer with a layer of four endothelium cells. (see figure 6) It is not known why this proliferation occurred. We hypothesize there may be some optical property of the Desemet's membrane which helps the cells to proliferate. This information may be useful in determining how to trigger human endothelium cells to regenerate *in-vivo* versus in culture.

The ANSI Z136.1 standard has three different methods for determining the maximum permissible exposure (MPE) for multiple pulse lasers. First, the MPE for any single pulse must not exceed the MPE. The second rule applies to the average power of

the laser pulses and generally only applies to lasers with a high duty cycle. Rule three is a thermal limit where the multi pulse correction factor, $n^{-0.25}$, where n is the number of pulses that occur in the group. Section 8.2.3.3 gives further details and recommends that the total exposure of 10 seconds MPE be the single pulse MPE divided by the number of pulses. The data presented herein do not support this methodology. In fact, single pulses incident upon the cornea that ranged from 11 to 343 seconds apart added to the total thermal energy in the surface of the cornea, even though they were spaced approximately 2.5 mm apart.

This study illustrates further investigation is needed to determine the time for thermal energy to be dissipated by the cornea, and exactly how multiple 1.54 micron pulses should be treated. The data extrapolated from the CO_2 laser in establishing the mid-infrared laser MPE limits may not be stringent enough. Multiple exposures sites across the cornea may cause the surface temperature of the cornea to increase with each successive pulse, narrowing the margin to non-reversible thermal injury. The mechanism causing the endothelium cells to proliferate in stratified layers needs to be examined. This knowledge may help in triggering human endothelium cells to proliferate *in-vivo*.

Acknowledgements

Table 1. Mean Corneal temperatures (°C) of Dutch belted rabbits before, during and 5 seconds after an 0.8 ms pulse from a 1540 nm laser exposure

Condition	No. of eyes	Mean	S.D.	Range
Normal(Mikesell 1978)	172	34.67	0.77	32.07 to 37.00
Baseline Exposure 1	13	35.33	0.72	34.31 to 36.59
Baseline Exposure 2	15	35.58	0.83	34.05 to 37.32
Peak Exposure One	13	64.64	7.37	55.67 to 79.21
Peak Exposure Two	15	62.37	5.47	54.39 to71.48
Peak Exposure Three	14	64.70	7.21	56.84 to 75.14
Baseline Exposure 3	14	35.79	0.87	34.52 to 37.14
Cool Exposure 1	13	36.37	1.09	34.40 to38.00
Cool Exposure 2	15	36.52	1.28	35.05 to 39.11
Cool Exposure 3	4	38.02	0.84	36.94 to 38.9
Δ T °C Baseline and Peak	42	28.41	6.41	18.88 to 42.62

Table 2. Mean time (sec) between exposure sets and mean change in temperature (ºC) between exposures sets

Condition	No. of eyes	Mean	S.D.	Range
Δ Time between Exp 1 & Exp 2 (sec)	13	31.38	36.74	12 to 140
Δ Time between Exp 2 & Exp 3 (sec)	14	40.57	53.82	11 to 203
Δ Time between Exp 1 & Exp 3 (sec)	12	73.33	94.79	25 to 343
ΔTemp baseline1-baseline2 (ºC)	13	0.19	0.37	-0.27 to 1.12
ΔTemp baseline2- baseline3 (ºC)	14	0.30	0.41	-0.21 to 1.02
ΔTemp baseline1- baseline3 (ºC)	12	0.51	0.43	-.26 to 1.1

Table 3. Pearson's Correlation Coefficient for time (sec) between exposures and temperature (^{o}C) change between baseline temperatures

Exposure Sets	Correlation Coefficient
Exposure 1 and 2	-0.41419
Exposure 2 and 3	0.566581
Exposure 1 and 3	0.274555
Exposure 1 and 2 and Exposure 2 and 3	0.436425
Time greater than 30 sec	0.492598

Table 4. Paired t-tests

Pairs	N	MEAN	SD	SE	95% CI Δ Lower	Upper	p-value
Peak Exp 1 – Peak Exp 3	12	-1.693	11.464	3.309	-8.977	5.591	0.619
Δ Time between Exp 1 & Exp 2 - Δ Time between Exp 2 & Exp 3 (sec)	12	-7.167	20.230	5.840	-20.020	5.687	0.245
Baseline1 - Baseline2	13	-0.191	0.368	0.102	-0.413	0.031	0.086
Baseline2 - Baseline3	14	-0.298	0.399	0.107	-0.528	-0.067	0.015*
Baseline1 - Baseline3	12	-0.511	0.432	0.125	-0.785	-0.237	0.002*
Baseline1 - Cool1	13	-1.044	0.664	0.184	-1.446	-0.643	0.001*
Baseline2 - Cool2	15	-0.943	0.826	0.213	-1.400	-0.486	0.001*
Baseline3 - Cool3	4	-1.723	0.466	0.233	-2.465	-0.981	0.005*
Baseline1 - Cool3	2	-2.563	0.437	0.309	-6.489	1.363	0.076**

*significant at an α=0.05 level

** not enough power to detect if there is a difference or not

Table 5. Measured and Calculated Δ T ºC

Condition	N	Mean	S.D.	Range
Δ T ºC Measured	42	28.41	6.41	18.88 to 42.62
Calculated Δ T ºC	54	16.33	0.77	14.60 to 17.37

Table 6. Measurements to Cornea as depicted in Figure 3

Description	Label on Figure 3	Length in microns
Thickness of cornea from epithelium to basal margin of Descemet's membrane in damaged tissue	L1	375.06
Thickness of damaged epithelium	L2	12.838
Thickness of damaged endothelium	L3	10.282
Thickness of cornea from basement of epithelium to Desemet's membrane in damaged tissue	L4	369.06
Thickness of Decemet's membrane in damaged tissue	L5	11.506
Thickness of Epithelium in normal tissue	L6	27.859
Thickness of Epithelium at edge of lesion	L7	11.506
Thickness of Epithelium at edge of lesion	L8	14.865
Thickness of Epithelium at edge of lesion	L9	11.884
Thickness of cornea in damaged tissue	L10	436.49
Thickness of damaged endothelium	L11	9.838
Thickness of damaged endothelium	L12	11.884
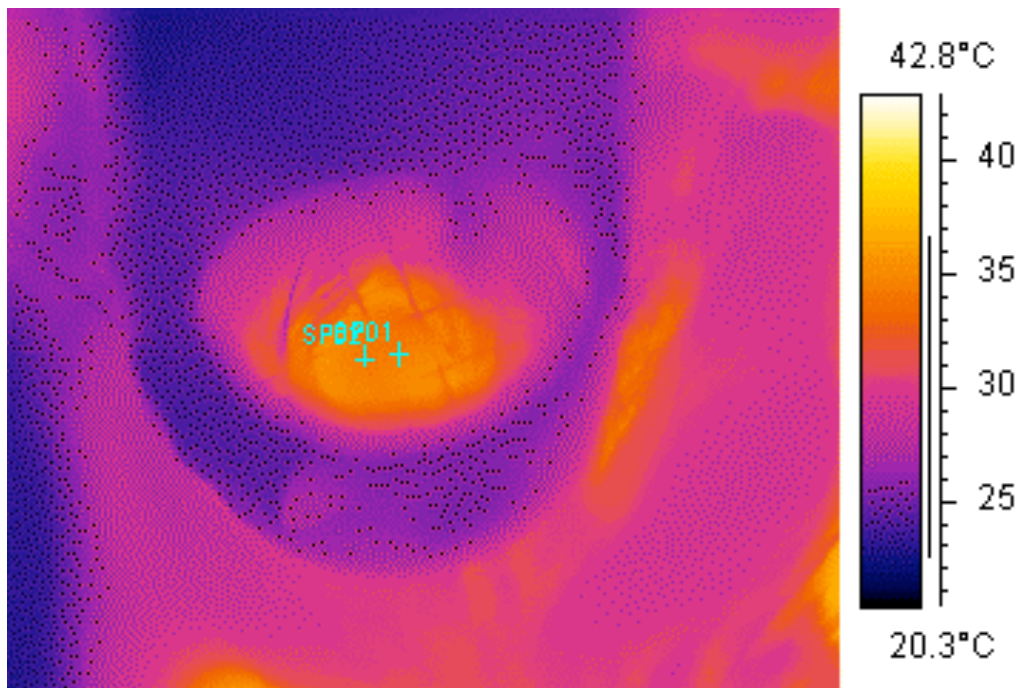
Figure 1. Thermal image depicting spot one, where the laser exposure occurred, and spot two, the reference spot.
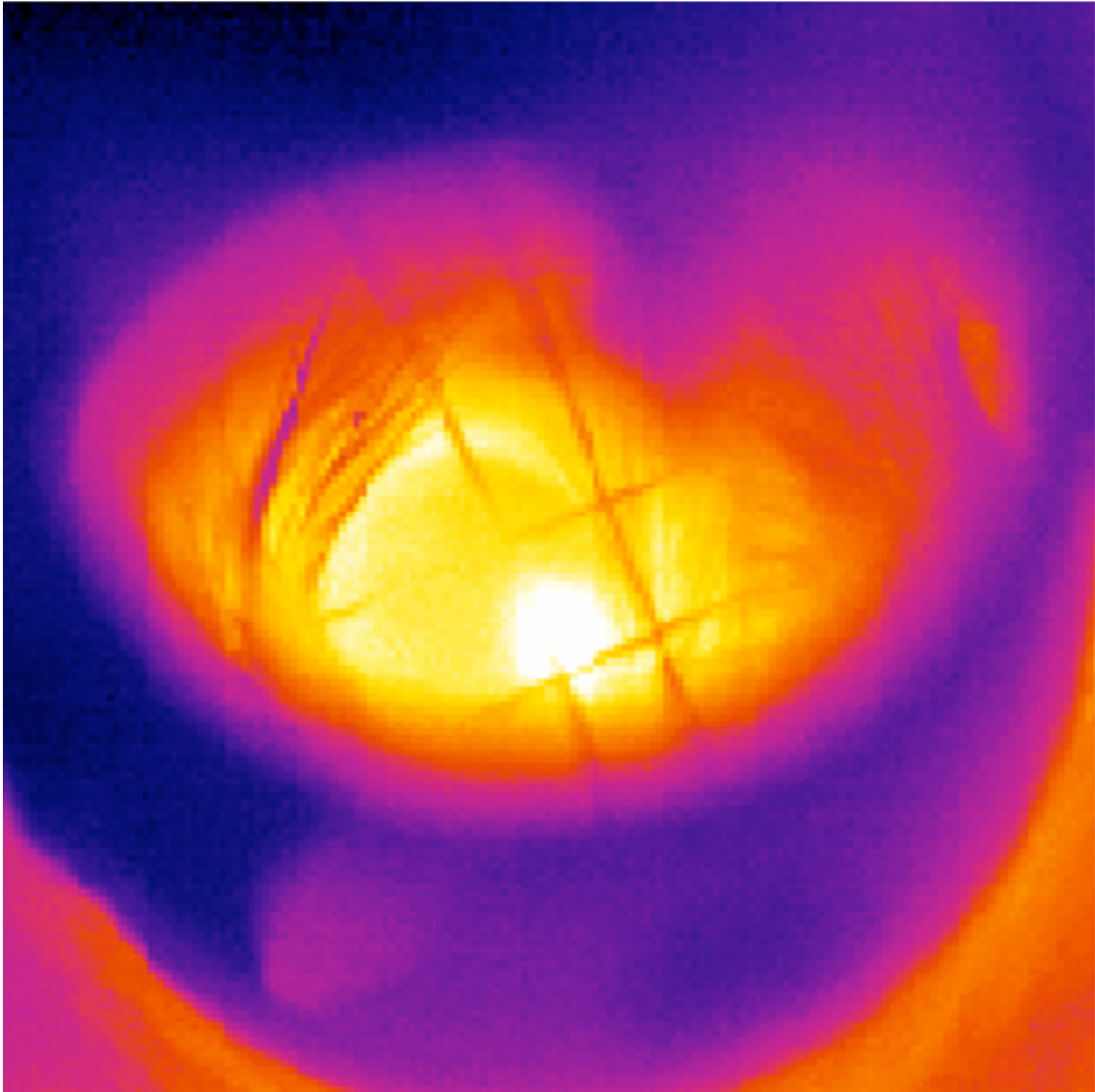
Figure2. Thermal image depicting the exposure
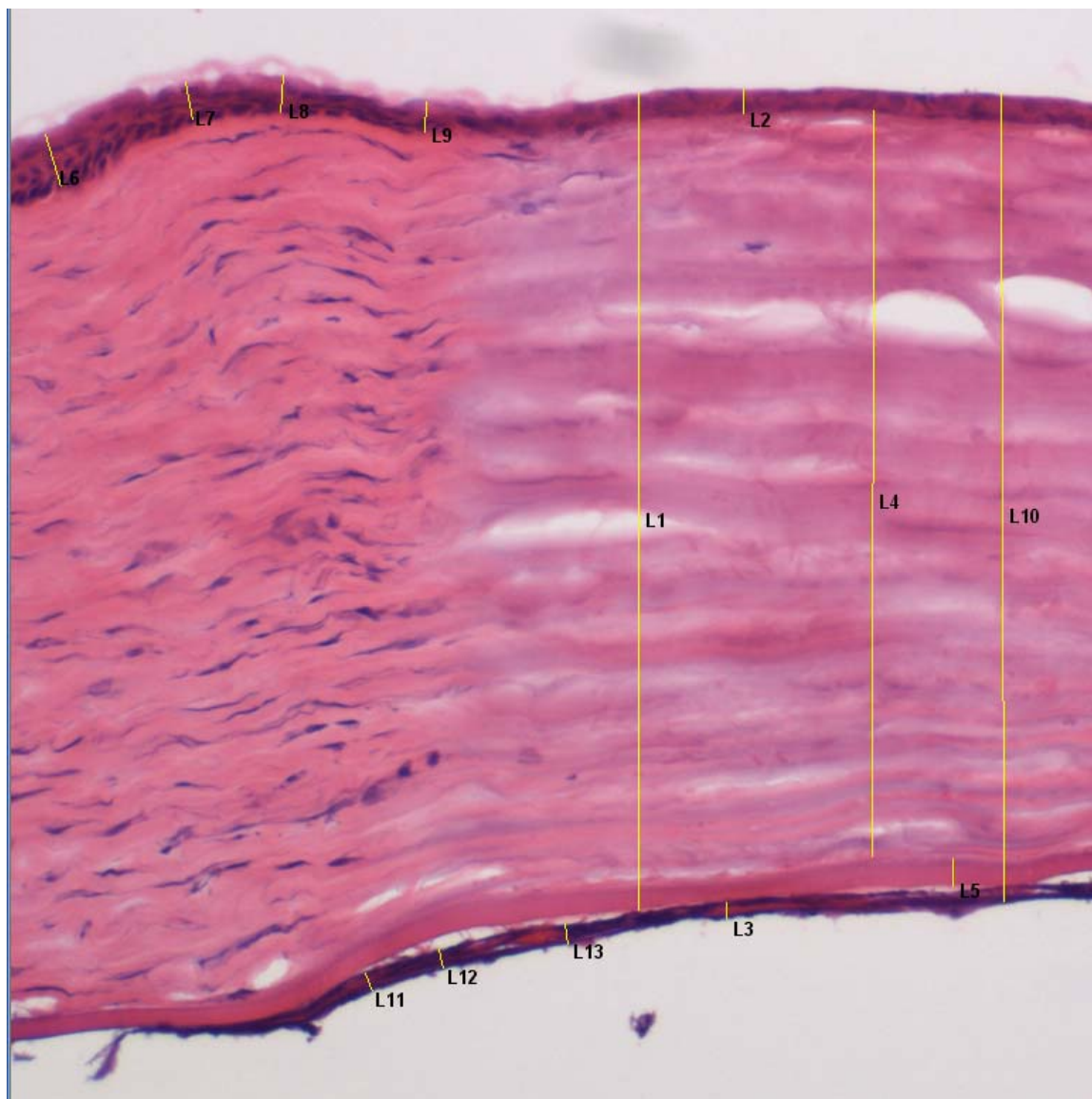
Figure 3. Representative sample of the exposures depicting the lesion and lesion measurements markings with labels corresponding to table 6
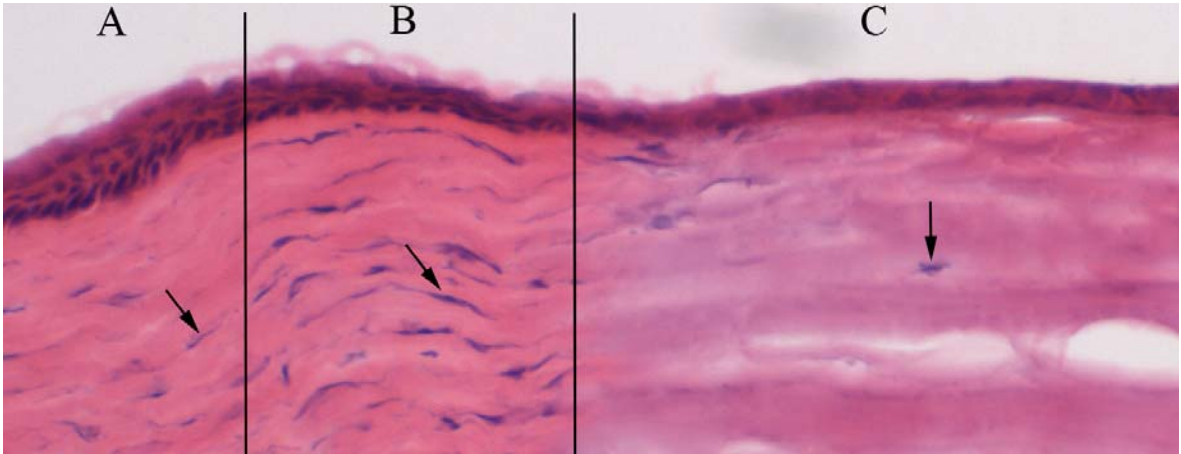
Figure 4. High magnification of lesion edge with epithelium and stroma. Zone A is a relatively normal area. Zone B is the region of stromal fibroblast proliferation. Zone C is the laser lesion. The arrows in each zone point to fibroblast nuclei.

Figure 5. Image of the lesion (10x) showing the endothelium layer in the lesion area to be thicker. The arrow points to the area depicted in Figure 6.
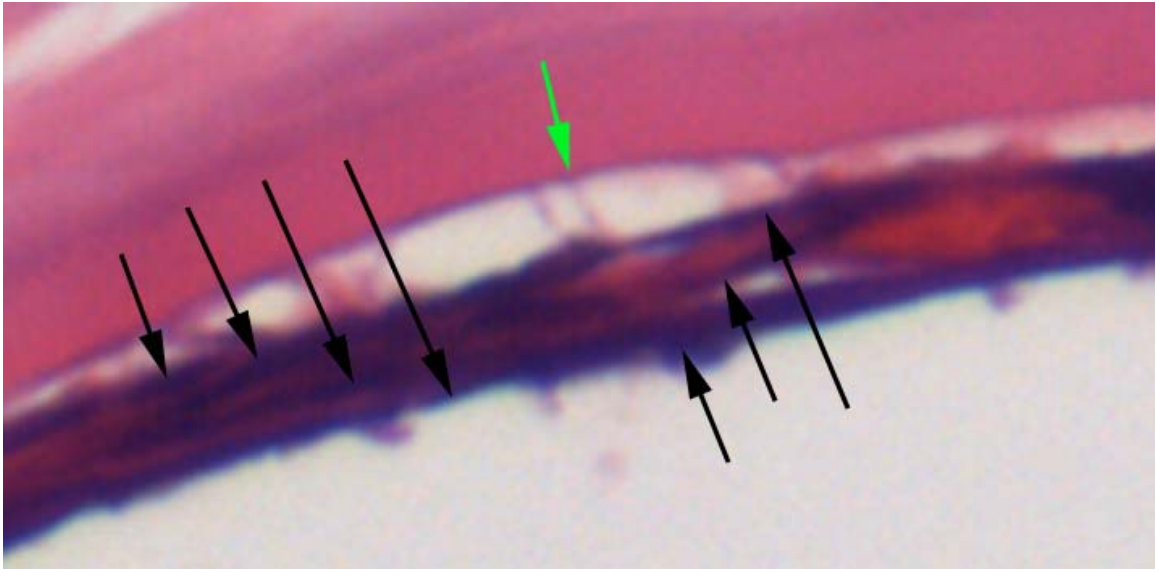
Figure 6. This is a higher magnification image of Figure 5 showing the laser induced

proliferation and stratification of the endothelial cells. The green arrow shows the basal

margin of Descemet's membrane. The black arrows point to different endothelial cell

nuclei. This is evidence of proliferation and stratification. The endothelial cells normally

exist as a single monolayer of cells beneath Descemet's membrane.

References Cited

Bargeron CB, McCally RL, Farrell RA. Calculated and measured endothelial temperature histories of excised rabbit corneas exposed to infrared radiation. Exp Eye Res 32: 241-50; 1981.

Buettner K. Effects of extreme heat and cold on human skin. I. Analysis of temperature changes caused by different kinds of heat application. J Appl Physiol 3: 691-702; 1951.

Clarke TF, Johnson TE, Burton MB, Ketzenberger B, Roach WP. Corneal injury threshold in rabbits for the 1540 nm infrared laser. Aviat Space Environ Med 73: 787-90; 2002.

McCally RL FR, Bargeron CB. Corneal Epithelial Damage Thresholds in Rabbits Exposed to Tm: YAG Laser Radiation at 2.02 um. Lasers in Surgery and Medicine 12: 598-603 1992.

Mikesell GW, Jr. Corneal temperatures--a study of normal and laser-injured corneas in the Dutch belted rabbit. Am J Optom Physiol Opt 55: 108-15; 1978.

Mishima S. Some Physiological Aspects of the Precorneal Tear Film. Arch Ophthalmol 73: 233-41; 1965.

Peppers NA, Vassiliadis A, Dedrick KG, Chang H, Peabody RR, Rose R, Zweng HC. Corneal Damage Thresholds for CO_2 Laser Radiation. Applied Optics 8: 377-381; 1969.

Rossi F, Pini R, Menabuoni L. Experimental and model analysis on the temperature
dynamics during diode laser welding of the cornea. J Biomed Opt 12: 014031;
2007.

Siegman AE SM, Johnston JTF. Choice of clip levels for beam width measurements
using knife-edge techniques. IEEE J Quantum Electron 27: 1098-1104; 1991.

Simanovskii D. MS, A. Irani, C. O'Connell-Rodwell, C. Contag, A. Schwettman, D.
Palanker. Cellular tolerance to pulsed heating. SPIE Proceedings, Laser-Tissue
Interactions XVI 5695: 1-5; 2005.

Chapter 7

Case Report: The Potential Hidden Hazards of an OPO Tunable Pumped Laser System

Abstract

Optical parametric oscillator (OPO) tunable laser systems from 1300 to 2200 nm have been introduced throughout the medical field due to their eye safe characteristics and ability to adjust to multiple wavelengths. We report on the unintended effects from a tunable laser system to rabbit corneas. While there was no visible damage post exposure, after enucleation and dissection, hemorrhaging was apparent in the globe. The bio-effects study was halted and evaluation of the tunable laser system revealed a cracked crystal and a resultant 1064 nm emission from the pump laser, rather than the desired 1540 nm wavelength. This incident illustrates the importance of protective eyewear shielding against all potential wavelengths, including the pump lasers, when operating OPO tunable laser systems.

Keywords: corneal, injury, safety.

Introduction

Recent advances in nonlinear optical crystals and solid state laser materials have created a new interest in tunable laser systems, particularly those utilizing optical parametric oscillators (OPOs). The optical parametric oscillator tunable laser system, hereafter referred to as an OPO laser system, is designed to emit coherent optical light. It can emit at almost any wavelength across a specified range by passing laser light from a diode pumped solid state laser through a nonlinear crystal [1,2,3]. The output beam produced by the OPO is indistinguishable from laser radiation in that both are coherent in space and time and monochromatic [1]. The OPO laser system falls into a larger class of tunable lasers, which also includes dye lasers, semi-conductor lasers, and excimer lasers. The OPO laser system, however, is the most promising of this group for clinical applications, and while these tunable laser systems are relatively new, they could possibly revolutionize laser use in medicine.

The ability to operate in the wavelength range from 1400 nm to 2200 nm is a particular benefit of OPO laser systems, as these output wavelengths are not a retinal hazard. Additionally, because OPO laser systems can be adjusted to more than one wavelength, a single laser system could potentially replace multiple lasers in a clinical practice. The OPO laser systems thereby provide an efficient and economical tool to the physician interested in providing a variety of treatments to patients. For example, the laser could be tuned to the wavelength ideal for the desired function of cutting epidermis, cauterizing blood vessels, or ablating skin. Finally, tunable lasers may help reduce the cost associated with maintaining multiple lasers within one practice. A physician could

utilize the same laser for multiple procedures, yet have only the costs associated with the purchase and maintenance of one laser system. Additionally, the space requirements of one laser system are far less than those of multiple systems.

For all the potential benefits and uses of the OPO laser system, there are also the inherent risks that come with any advancing technology. While lasers operating at 1400 nm or greater are marketed as "eye safe, this term may be a misnomer. A safety hazard may exist even if the output beam is below the ANSI maximum permissible exposure limits. This can occur if the beam is modified using focusing lenses or if it is deliberately stared into [4]. The pumping lasers associated with the OPO laser system can also pose a safety risk. If the pumping laser is in the near infrared (700 nm to 1400 nm) personnel accidentally exposed would neither see the beam nor feel the damage occurring to the retina. Near infrared light is transmitted by the cornea and lens then absorbed by the retina, an area devoid of pain receptors. All OPO laser exposure accidents found in the literature are from the known output range of the OPO laser and are not caused by the pumping laser [4,5]. The incident discussed in this case report involved exposure to our research subjects from the input or pump laser in an OPO tunable laser system producing output within the retinal hazard region (1064 nm). This case report illustrates the need for continual evaluation of the potential risks and underlying hazards associated with the advancement of laser technology.

Study Design/Patient and Methods

We report on the unintended effects (vitrous hemorrhage) on *in-vivo* rabbit eye exposures to a 1540 nm OPO tunable laser system. The objective of the study was to

determine the *in-vivo* (rabbit) median effective dose (ED_{50}) of an OPO laser system to cause visible damage to the cornea from a 1540 nm single pulse exposure.

Animals

Four male Dutch-belted rabbits were obtained from Covance Inc., Princeton, NJ with ages that ranged from 1-2 years old and weights from 2-3 kg. All animals were housed in accordance with the *Guide for the Care and Use of Laboratory Animals* [6] and participated in an environmental enrichment program at the Uniformed Services University of Health Sciences (USUHS). The procedures were performed under an animal use protocol approved by the Institutional Animal Care and Use Committee (IACUC) at USUHS. USUHS is fully accredited by the American Association for Accreditation of Laboratory Animal Care (AAALAC), International.

Rabbits were maintained under anesthesia throughout exposure. Buprenorphine (0.05 mg/kg, IM, Reckitt & Colman Pharmaceuticals, Inc., Richmond, VA)) was administered intramuscularly for analgesia prior to recovery from anesthesia and at 12-hour intervals post procedure. Following the study, rabbits were euthanized using Sodium Pentobarbital 390 mg/ml (1 ml/rabbit, Euthasol, Virbac AH, Inc, Fort Worth, TX) administered by intracardiac injection in accordance with the American Veterinary Medical Association 2000 Panel on Euthanasia [7] and the approved protocol.

Corneal laser exposures involved placing rabbits on a platform in sternal recumbancy. An ocular speculum was used to keep the rabbit's eye open during exposures. Proper positioning was determined with the use of a co-linear HeNe alignment beam. Three laser exposures per cornea were conducted in a horizontal linear fashion moving from medial to lateral on both eyes.

Laser

An experimental OPO laser system, specifically designed for corneal experiments, produced 16 ns single pulses at approximately 1 Hz. The input or pump laser was a 1064 nm Nd:YAG laser. The laser was equipped with the safety devices specified by ANSI Z136.1-2000, section 4.3 for a class 4 laser [8]. The OPO wavelength output could be manually adjusted from 1400 nm to 2000 nm by manually re-positioning the Potassium dihydrogen phosphate nonlinear crystal. The system could be operated in single pulse or multiple pulse modes.

The output beam was focused on the subject's cornea with a 200 mm lens (BK-7 lens material, LA1708, Newport, Irvine CA). The energy output was measured using a Molectron EPM-2000 meter and a J25 energy detector (Coherent, Santa Clara CA). Pulse duration was determined by a Germanium photon detector (PDA 255, Thor Labs, Newton, NJ) connected to a Tektronix TDS 644B (Richardson, TX) digitizing oscilloscope. The exposure was a single 16 ns pulse with a spot size of 0.3 mm^2.

Results

There was no visible damage to the cornea, either immediately or 24 hours post-exposure to the cornea. Upon viewing the rabbit's eyes with an ophthalmoscope and slit lamp, there appeared to be lesions on the retina visible 8 hours post exposure. The animals were subsequently euthanized. After enucleating and dissecting the eyes, hemorrhaging was apparent in the posterior globe consistent with a vitreoretinal hemorrhage. There were no visible lesions to the cornea when viewed under the

dissection microscope that would be consistent with 1540 nm energy absorption [Fig 1A].

When the intended effects were not produced [Fig 1B], the cornea injury study was halted. An evaluation of the laser system revealed that the OPO's nonlinear crystal was cracked, which resulted in a direct emission of the pumping laser beam at 1064 nm. Four rabbits were utilized in this experiment before the study was halted. The USUHS Lab Animal Medicine Veterinarian and the IACUC was notified of the unexpected morbidity resulting from the study.

All personnel in the laboratory were wearing safety goggles that provided protection from both the intended output wavelength of 1540 nm and the 1064 nm source pumping laser, so no operators were harmed over the course of the experiment.

Operator Actions

In this case, the OPO laser system did not produce the intended effect due to output of the incorrect wavelength. When the expected results did not occur, the operators increased the energy in an attempt to produce the effect, mistakenly thinking that the tissue was more robust than expected. Further discussion with the operators revealed that they felt the output of the laser system may have been reduced due to corrosion or misalignment.

Discussion

The design of the laser system used in this study did not allow the operator to view the nonlinear crystal component of the OPO to ensure that its integrity was not compromised, since the operator could then be exposed to the pumping laser beam as well. Wavelength measurement before the procedure did not prevent the OPO laser

system from malfunctioning during the procedure. During the repair of the OPO laser system, the replacement crystal broke after three individual firings.

While the pumping laser was known to be a 1064 nm Nd:YAG laser, the output wavelength beam could only be determined through use of a monochrometer, an instrument not typically available in a clinical setting, as these devices are typically cost prohibitive. Additionally, the output beam of the OPO laser system was verified by the manufacturer via monochrometer during installation.

This experimental OPO laser system was not equipped with any safety devices to shut off the beam if the output wavelength was not as specified. A solution to this situation might be to install optics that are opaque to wavelengths less than 1400 nm (retinal hazard region), so that if the system failed, no emission would result.
It was by fortunate chance that goggles were worn that covered both the input and output wavelengths, as the 1064 nm wavelength is absorbed by the retina and may have caused permanent loss of vision. Additionally, because the 1064 nm wavelength is in the near infrared range of the spectrum, the operator or patient would not be able to see the laser or even feel the effects during an exposure.

When using any tunable laser system, the operators should be aware of all possible wavelengths of emission, including the pumping wavelength and any other incidental harmonics. While ANSI Z136.1-2000 does have provisions for multiple wavelength lasers, this section refers to lasers that are intended to put out multiple wavelengths simultaneously, and not tunable laser systems with one intended output wavelength [8].

Many of the laser eye injuries reported in the literature result from the operator not wearing the protective safety goggles or wearing the incorrect goggles for the wavelength

being utilized [5]. The OPO tunable laser system adds a new dimension to these preventable eye injuries by further complicating the selection of proper eyewear. The OPO laser system has multiple wavelengths that an operator can specify and thus be exposed to, as well as the added possibility of exposure to the input laser. While manufacturers state on the warning label of the laser system that the input pump laser is a possible wavelength, operators do not typically wear goggles for all possible wavelengths of the laser system, only for the intended or set output wavelength they are currently using.

Conclusion

This case report illustrates the need for continual evaluation of the potential risks and underlying hazards associated with the advancement of laser technology. The operators of an OPO tunable laser system in a lab or clinical setting may need to use personal protective measures for the input or source laser wavelength in addition to the desired output wavelength unless engineering controls are in place. The combination of using personal protective measures covering both wavelengths and using engineering controls will allow for the safe use of the OPO laser system for both the operator and patient.

Acknowledgements

Fig. 1. A. Expected presentation from a 1540 nm exposure; 3 visible lesions. B. Expected presentation of the cornea from a 1064 nm exposure; no visible lesions.

References Cited

[1] Duarte FJ. Tunable laser applications. New York: Marcel Dekker; 1995.

[2] Giordmaine JA, Miller RC. Tunable coherent parametric oscillation in $LiNbO_3$ at optical frequencies. Phys Rev Lett 1965; 14: 973-6.

[3] Kingston RH. Parametric amplification and oscillation at optical frequencies. Proc IRE 1962; 50: 472.

[4] Sliney DH. Following standards and using appropriate safety equipment can help eliminate the risk of eye injuries during laser use. OE Magazine 2001; 1: 34-6.

[5] Sliney DH. Ocular injuries from laser accidents. In: Stuck BE, Belkin M, editors. Proceedings SPIE 2674 Laser-inflicted eye injuries: epidemiology, prevention and treatment, Washington; 1996, p. 25-33.

[6] National Research Council. Guide for the Care and Use of Laboratory Animals. Washington (DC): National Academy Press; 1996.

[7] American Veterinary Medical Association. Report of the AVMA panel on euthanasia. J Am Vet Med Assoc 2001. 218: 669-96.

[8] American National Standards Institute. ANSI Z136.1-2000, American National Standard for safe use of lasers. Laser Institute of America, Orlando, FL; 2000.

Chapter 8

Conclusion

CHAPTER 8: CONCLUSION

Since the development of lasers a wide body of research has been conducted to understand the parameters involved in injury to both ocular and dermal tissue. This study looked at the bio-effects of 1540 nm laser to ocular tissue. Laser safety standards and regulations have been developed nationally, internationally and by the armed services to promote the safe design and use of lasers. Despite their existence, accidental eye injuries from lasers still occur. While these accidental exposures add to our knowledge and understanding of laser bio-effect to humans, without knowledge of all the parameters involved it is difficult to compile this information into a useable epidemiologic study. Therefore, research is primarily conducted using live animal models.

In this research, alternatives to live animals in research using lasers was conducted with the use of both *in-vitro* and *ex-vivo* rabbit models and compared their median effective dose (ED_{50}) to the reported median effective dose of the reported *in-vivo* model with analogous laser parameters. It was found that the ED_{50} of both the *in-vitro* (21.24 J/cm^2) and *ex-vivo* (30.86 J/cm^2) models were substantially less than the reported *in-vivo* (56 J/cm^2) model's ED_{50}. This difference in the ED_{50}'s may be explained by the robustness of the tissue models. The alternative animal models ED_{50}'s were correlated to the *in-vivo* with a fixed factor. The fixed factors may allow the use of the alternative models as a rapid screening of laser tissue interactions. The tissue interactions of both the *in-vitro* and *ex-vivo* models were similar showing necrosis and ablation of tissue from the epithelial layer into the deeper stromal layers. Both models showed a proliferation of epithelial cells indicating the healing process of the cornea models.

Looking at the tissue laser interactions in more detail the *ex-vivo* model was utilized to look at the difference of pulse duration and spot size, as well as make comparisons of using standard histomorphology versus immunohistological analyses. From this research we were able to show that the spot size and pulse duration produced significant differences in mean depth, diameter and area of the laser exposure on the tissue. The comparison of the standard histomorphology versus immunohistological analyses indicated the same mean depth and diameter of the laser exposure could be determined, but the proportion of area affected by the laser exposure was statistically different for each pulse width and spot size. This difference indicates the two analyses should be used in concert to determine tissue damage post exposure

The mechanism for tissue damage for the 1540 nm wavelength has been described as a thermal mechanism. This mechanism was explored using thermal infrared imaging to determine the measured change in temperature of the *in-vivo* cornea during a laser exposure sequence. The level of energy absorption in the ocular tissue is critical because as more absorption occurs, the more energy is converted into heat. It is temperature elevation and duration that determine the extent of tissue damage. Thermal tissue damage is caused within a few microseconds and is the most common form of optical damage on the battlefield (Small 2007).

We found the mean thermal temperature change of $28.41^{o}C$, ranging from 18.88 to 42.62 ^{o}C resulted in visible injuries This temperature change from our established mean baseline temperature of 35.33 ^{o}C did not meet the critical temperature of 67 ^{o}C for denaturizing protein as related by Peppers (Peppers et al. 1969). When we calculated the temperature change using the radiant exposure and Buettner's equation, the calculated

change in temperature was 16.33 $^{\circ}$ C (14.6 to 17.37 $^{\circ}$ C) (Buettner 1951). This indicates

that there may be a combination of models needed to explain the thermal component of

the temperature response and damage mechanism for ocular tissue at this pulse duration.

The laser exposures were done in serial exposures across the eye. The data indicates the

eye remained heated from one exposure to the next by a mean temperature of 1.08 $^{\circ}$C

higher than before the exposure, which was significant at α=0.05 level. Histology

indicated all the exposures caused damage to the maximum depth of the rabbit cornea and

therefore we could not determine if depth of damage increased with each successive laser

exposure.

Histology also showed that the keratocytes on the periphery of the lesion edge

were activated and proliferating compared to the healthy tissue that was unaffected by the

exposure. The keratocytes within the exposure showed necrosis. The normal single cell

layer of endothelial cells within the region of the laser exposure showed a stratified

proliferation of up to four layers of endothelial cells. While rabbit endothelial cells

proliferate *in-vivo*, unlike human endothelial cells, they do not stratify into layers.

Investigation into the mechanism triggering the endothelial cellular response of this laser

tissue interaction may help in determining how to trigger human cells to proliferate *in-

vivo*.

These papers indicate that the use of alternative models may be viable in use as a

screening tool for future studies of bio-effects from lasers with ocular tissue. The use of

these alternative models may help minimize the use of live animal models in this

research. Since each laser wavelength and parameter of the lasers changes the dynamics

involved with laser safety, it is important to try to minimize the use of live animal models

while providing critical information to fill the research gap of all lasers bio-effects and determine appropriate safety standards.

The application of the laser has evolved from when it was first introduced. These applications include medicine, industry, laboratory research, entertainment, and the military. The situation regarding the potential for laser injuries in military is different than in civilian settings. Lasers are very commonly used in the military outdoors at very long ranges and most laser-associated military activities involve the beaming of targets that usually contain people, some of whom are using binoculars and other magnifying optics, making their eyes vulnerable over many kilometers (Barkana and Belkin 2000).

In order to protect from laser eye injuries the use of wavelength specific filters are utilized. In order to determine the correct goggles to wear, the operator must determine the parameters of the laser he is using or may be exposed to. In medicine and industry this task should be simple since all the parameters are known. Yet, human laser eye incidents are still reported due to not using protective goggles or using the incorrect goggles. In the military environment determining the appropriate eye protection is not as easy since the person exposed may not know all the parameters of the laser threats possible.

The final manuscript details an incident that occurred in the course of this research. The research started with an optical parametric oscillator (OPO) tunable laser systems that ranged from 1300 to 2200 nm. The pump source of this laser system was a 1064 nm Nd:YAG laser. Lasers of this type are marketed as eye safe because the pump laser which can damage the retina is transformed into a wavelength that affects the cornea. Since the cornea can repair superficial damage industry markets it as 'eye safe.'

In our case our OPO laser system had a cracked crystal and was emitting the 1064 nm wavelength in concert to the 1540 nm wavelength it was set to. The operators were not injured because they were wearing goggles that happened to also protect from this wavelength. This case illustrates the difficulty of wearing the appropriate protective goggles in the modern age of lasers. It also illustrates how difficult it will become for military personnel who may be exposed to a wide range of lasers used on the battlefield for target designation, range finding and threat systems.

In conclusion, this research shows the usefulness of alternative models in exploring the bio-effects of laser tissue interaction. Further research is warranted into looking at using alternative models at different wavelengths and in human *in-vitro* and *ex-vivo* models. The thermal component of tissue damage requires further exploration to determine if serial exposures may cause more damage to the tissue. Additionally the mechanism for triggering endothelial cell proliferation and stratification requires further research to determine if there is a way to trigger human endothelial cell proliferation *in-vivo*.

Bibliography

ANSI. 2000. *Z136.1-2000 American National Standard For Safe Use Of Lasers* New York: American National Standards Institute.

ASPCA. 2005. Animal Testing: Things Are Changing Because Of New Technology. In *Real Issues*: ASPCA website.

Bargeron, C. B., O. J. Deters, R. A. Farrell, and R. L. McCally. 1989. Epithelial Damage In Rabbit Corneas Exposed To Co2 Laser Radiation. *Health Phys* 56, no. 1: 85-95.

Bargeron, C. B., R. L. McCally, and R. A. Farrell. 1981. Calculated And Measured Endothelial Temperature Histories Of Excised Rabbit Corneas Exposed To Infrared Radiation. *Exp Eye Res* 32, no. 2: 241-50.

Barkana, Y. and M. Belkin. 2000. Laser Eye Injuries. *Surv Ophthalmol* 44, no. 6: 459-78.

Brinkmann, R., G. Huttmann, J. Rogener, J. Roider, R. Birngruber, and C. P. Lin. 2000. Origin Of Retinal Pigment Epithelium Cell Damage By Pulsed Laser Irradiance In The Nanosecond To Microsecond Time Regimen. *Lasers Surg Med* 27, no. 5: 451-64.

Buettner, K. 1951. Effects of extreme heat and cold on human skin. I. Analysis Of Temperature Changes Caused By Different Kinds Of Heat Application. *J Appl Physiol* 3, no. 12: 691-702.

Cain CP, Noojin GD. 1996. *A Comparison Of Various Probit Methods For Analyzing Yes/No Data On A Log Scale*. USAF AL/OE-TR-1996-0102.

Carroll, Lisa and Tatyana R. Humphreys. 2006. Laser-Tissue Interactions. *Clinics in Dermatology* 24: 2-7.

Clark, Krystyn. 2004. The Delphi Technique Used In Laser Incident Surveillance, USUHS.

Clarke, T. F., T. E. Johnson, M. B. Burton, B. Ketzenberger, and W. P. Roach. 2002. Corneal Injury Threshold In Rabbits For The 1540 Nm Infrared Laser. *Aviat Space Environ Med* 73, no. 8: 787-90.

Daniels, J. T., G. Geerling, R. A. Alexander, G. Murphy, P. T. Khaw, and U. Saarialho-Kere. 2003. Temporal And Spatial Expression Of Matrix Metalloproteinases During Wound Healing Of Human Corneal Tissue. *Exp Eye Res* 77, no. 6: 653-64.

Daniels, J. T. and P. T. Khaw. 2000. Temporal Stimulation Of Corneal Fibroblast Wound Healing Activity By Differentiating Epithelium In Vitro. *Invest Ophthalmol Vis Sci* 41, no. 12: 3754-62.

Endangered Species Act Of 1973. 1973.

Esquenazi, S., J. He, N. G. Bazan, and H. E. Bazan. 2005. Comparison Of Corneal Wound-Healing Response In Photorefractive Keratectomy And Laser-Assisted Subepithelial Keratectomy. *J Cataract Refract Surg* 31, no. 8: 1632-9.

Fini, M. E. and B. M. Stramer. 2005. How The Cornea Heals: Cornea-Specific Repair Mechanisms Affecting Surgical Outcomes. *Cornea* 24, no. 8 Suppl: S2-S11.

Finney, D. J. 1971. *Probit analysis*. Cambridge [Eng.]: University Press.

Fleischauer, Eric. 2005. Blinding Light As A Weapon: Lasers Pose Threat To Airplane Pilots *Decatur Daily News*, Jan 7 2005

Framme, C., G. Schuele, J. Roider, R. Birngruber, and R. Brinkmann. 2004. Influence Of Pulse Duration And Pulse Number In Selective Rpe Laser Treatment. *Lasers Surg Med* 34, no. 3: 206-15.

Freund, D. E., R. L. McCally, R. A. Farrell, S. M. Cristol, N. L. L'Hernault, and H. F. Edelhauser. 1995. Ultrastructure In Anterior And Posterior Stroma Of Perfused Human And Rabbit Corneas. Relation To Transparency. *Invest Ophthalmol Vis Sci* 36, no. 8: 1508-23.

Fyffe, James. 2005. Corneal Injury To Ex-Vivo Eyes Exposed To A 3.8 Micron Laser, USUHS.

Ham WT, Mueller HA. 1991. Ocular Effects Of Laser Infrared Radiation. *J. Laser App* 3, no. 3H: 19-21.

Heisterkamp, A., T. Mamom, O. Kermani, W. Drommer, H. Welling, W. Ertmer, and H. Lubatschowski. 2003. Intrastromal Refractive Surgery With Ultrashort Laser Pulses: In Vivo Study On The Rabbit Eye. *Graefes Arch Clin Exp Ophthalmol* 241, no. 6: 511-7.

ICRC. 13 October 1995 1995. *Protocol On Blinding Laser Weapons (Protocol Iv To The 1980 Geneva Convention)*. United Nations CCW/CONF.I /7. Accessed 1 September 2005. Available from http://www.icrc.org/ihl.nsf/0/49de65e1b0a201a7c125641f002d57af?OpenDocument.

Isnard, N., F. Bourles-Dagonet, L. Robert, and G. Renard. 2005. Studies On Corneal Wound Healing. Effect Of Fucose On Iodine Vapor-Burnt Rabbit Corneas. *Ophthalmologica* 219, no. 6: 324-33.

Jane's international defense review. 2005. Jane's.

Jester, J. V., A. Budge, S. Fisher, and J. Huang. 2005. Corneal Keratocytes: Phenotypic And Species Differences In Abundant Protein Expression And In Vitro Light-Scattering. *Invest Ophthalmol Vis Sci* 46, no. 7: 2369-78.

Ketzenberger, B., T. E. Johnson, Y. A. Van Gessel, S. P. Wild, and W. P. Roach. 2002. Study Of Corneal Lesions Induced By 1,318-Nm Laser Radiation Pulses In Dutch Belted Rabbits (Oryctolagus Cuniculus). *Comp Med* 52, no. 6: 513-7.

Kuo, I. C. 2004. Corneal Wound Healing. *Curr Opin Ophthalmol* 15, no. 4: 311-5.

Kurtz, R. M., C. Horvath, H. H. Liu, R. R. Krueger, and T. Juhasz. 1998. Lamellar Refractive Surgery With Scanned Intrastromal Picosecond And Femtosecond Laser Pulses In Animal Eyes. *J Refract Surg* 14, no. 5: 541-8.

Lasers And Optical Radiation. 1982. In *INTERNATIONAL PROGRAMME ON CHEMICAL SAFETYENVIRONMENT HEALTH CRITERIA 23*:40: the United Nations Environment Programme, the International Labour Organisation, and the International Radiation Protection Association.

Markov, Vladimir. 30 Sep 04. 2004. *Eye-Safe Ladar Laser Transmitter*. NAVY. Accessed 8 May 2007. Abstract. Available from http://www.dodsbir.net/selections/abs011/navyabs011.htm.

McCally, R. L., C. B. Bargeron, W. R. Green, and R. A. Farrell. 1983. Stromal Damage In Rabbit Corneas Exposed To Co2 Laser Radiation. *Exp Eye Res* 37, no. 6: 543-50.

McCally, R. L., R. A. Farrell, and C. B. Bargeron. 1992. Cornea Epithelial Damage Thresholds In Rabbits Exposed To Tm:Yag Laser Radiation At 2.02 Microns. *Lasers Surg Med* 12, no. 6: 598-603.

Mikesell, G. W., Jr. 1978. Corneal Temperatures--A Study Of Normal And Laser-Injured Corneas In The Dutch Belted Rabbit. *Am J Optom Physiol Opt* 55, no. 2: 108-15.

Mil-Std882C. 1993. Systems Safety Program Requirements, ed. DoD, Military Standard 882C: US Department of Defense.

Mil-Std1425A. 1991. Safety Design Requirements For Military Lasers And Associated Support Equipment, ed. DoD, Military Standard 1425A: US Department of Defense.

Mishima, S. 1965. Some Physiological Aspects Of The Precorneal Tear Film. *Arch Ophthalmol* 73: 233-41.

Miyamoto, T., S. Saika, A. Yamanaka, Y. Kawashima, Y. Suzuki, and Y. Ohnishi. 2003. Wound Healing In Rabbit Corneas After Photorefractive Keratectomy And Laser In Situ Keratomileusis. *J Cataract Refract Surg* 29, no. 1: 153-8.

Mulholland, B., S. J. Tuft, and P. T. Khaw. 2005. Matrix Metalloproteinase Distribution During Early Corneal Wound Healing. *Eye* 19, no. 5: 584-8.

National Environmental Policy Act Of 1973. 1973.

NATO. 1988. Evaluation And Control Of Laser Hazards On Military Ranges., Mons, Belgium: NATO Standardization Agreement (STANAG) 3606: North Atlantic Treaty Organization.

NEI. 2007. *Facts About The Cornea And Corneal Disease*. Accessed 15 August 2005. website. Available from http://www.nei.nih.gov/health/cornealdisease/index.asp#0.

Netto, M. V., R. R. Mohan, R. Ambrosio, Jr., A. E. Hutcheon, J. D. Zieske, and S. E. Wilson. 2005. Wound Healing In The Cornea: A Review Of Refractive Surgery Complications And New Prospects For Therapy. *Cornea* 24, no. 5: 509-22.

Ojeda, J. L., J. A. Ventosa, and S. Piedra. 2001. The Three-Dimensional Microanatomy Of The Rabbit And Human Cornea. A Chemical And Mechanical Microdissection-Sem Approach. *J Anat* 199, no. Pt 5: 567-76.

Peppers, N. A., A. Vassiliadis, K. G. Dedrick, H. Chang, R. R. Peabody, R. Rose, and H. C. Zweng. 1969. Corneal Damage Thresholds For Co2 Laser Radiation. *Applied Optics* 8, no. 2: 377-381.

Profio, A. E. and D. R. Doiron. 1987. Transport Of Light In Tissue In Photodynamic Therapy. *Photochem Photobiol* 46, no. 5: 591-9.

Rossi, F., R. Pini, and L. Menabuoni. 2007. Experimental And Model Analysis On The Temperature Dynamics During Diode Laser Welding Of The Cornea. *J Biomed Opt* 12, no. 1: 014031.

Rossi, F., R. Pini, L. Menabuoni, R. Mencucci, U. Menchini, S. Ambrosini, and G. Vannelli. 2005. Experimental Study On The Healing Process Following Laser Welding Of The Cornea. *J Biomed Opt* 10, no. 2: 024004.

Russell, W. M. S. and R. L. Burch. 1959. *The Principles Of Humane Experimental Technique*. Springfield, Ill.,: C.C. Thomas.

Schaffer, CJ, L Reinisch, SL Polis, GP Stricklin, and LB Nanney. 1997. Comparisons Of Wound Healing Among Excisional, Laser Created, And Standard Thermal Burns In Porcine Wounds Of Equal Depth. *Wound repair and regeneration* 5, no. 1: 52-61.

Schawlow, Arthur L. 1969. *Lasers And Light; Readings From Scientific American*. San Francisco,: W. H. Freeman.

Schuele, G., M. Rumohr, G. Huettmann, and R. Brinkmann. 2005. Rpe Damage Thresholds And Mechanisms For Laser Exposure In The Microsecond-To-Millisecond Time Regimen. *Invest Ophthalmol Vis Sci* 46, no. 2: 714-9.

Shiner, Bill. 2004. Fiber frenzy. In *Industrial Laser Solutions*

Siegman, AE, MW Sasnett, and JTF Johnston. 1991. Choice Of Clip Levels For Beam Width Measurements Using Knife-Edge Techniques. *IEEE J Quantum Electron* 27: 1098–1104.

Slatter, Douglas H. 1990. *Fundamentals Of Veterinary Ophthalmology*. Philadelphia, PA: Saunders.

Sliney, David H. and Myron Wolbarsht. 1980. *Safety With Lasers And Other Optical Sources : A comprehensive handbook*. New York: Plenum Press.

Small, Lisa A. 2007. Blinding laser weapons: It is time for the international Community To Take Off Its Blinders.

SPIE. 1995. Spie Milestone Series: Selected Papers On Laser Safety, ed. Brian J. Thompson and David H. Sliney, MS 117 SPIE Optical Engineering Press.

Steen, W. M. 1998. Brief History Of Laser. In *Laser Materials Processing*, 2nd Ed. : University of Liverpool.

Sugar, A. 2002. Ultrafast (Femtosecond) Laser Refractive Surgery. *Curr Opin Ophthalmol* 13, no. 4: 246-9.

van Gemert, M. J., S. L. Jacques, H. J. Sterenborg, and W. M. Star. 1989. Skin optics. *IEEE Trans Biomed Eng* 36, no. 12: 1146-54.

Vogel, A., S. Busch, K. Jungnickel, and R. Birngruber. 1994. Mechanisms Of Intraocular Photodisruption With Picosecond And Nanosecond Laser Pulses. *Lasers Surg Med* 15, no. 1: 32-43.

Vogel, A., M. R. Capon, M. N. Asiyo-Vogel, and R. Birngruber. 1994. Intraocular Photodisruption With Picosecond And Nanosecond Laser Pulses: Tissue Effects In Cornea, Lens, And Retina. *Invest Ophthalmol Vis Sci* 35, no. 7: 3032-44.

Xu, M. and R. R. Alfano. 2005. Fractal Mechanisms Of Light Scattering In Biological Tissue And Cells. *Opt Lett* 30, no. 22: 3051-3.

Appendix C – *Ex-Vivo* Morphologic Summaries

H&E width of lesion

t-test   Tuesday, February 28, 2006, 16:54:12

Data source: Data 1 in Notebook

Normality Test: Passed (P = 0.247)

Equal Variance Test: Failed (P = 0.035)

Test execution ended by user request, Rank Sum Test begun

Mann-Whitney Rank Sum Test   Tuesday, February 28, 2006, 16:54:12

Data source: Data 1 in Notebook

Group	N	Missing
Col 1	10	0
Col 2	10	0

Group	Median	25%	75%
Col 1	552.714	549.030	557.645
Col 2	163.962	162.344	165.894

T = 155.000 n(small)= 10 n(big)= 10 (P = <0.001)

The differences in the median values among the two groups are greater than would be expected by chance; there is a statistically significant difference (P = <0.001)

H&E depth of lesion

t-test   Tuesday, February 28, 2006, 17:02:44

Data source: Data 1 in Notebook

Normality Test: Failed (P = 0.013)

Test execution ended by user request, Rank Sum Test begun

Mann-Whitney Rank Sum Test   Tuesday, February 28, 2006, 17:02:44

Data source: Data 1 in Notebook

Group N   Missing
Col 3   10   0
Col 4   10   0

Group Median   25%   75%
Col 3   701.303   693.630   714.832
Col 4   415.496   413.863   416.333

T = 155.000 n(small)= 10 n(big)= 10 (P = <0.001)

The differences in the median values among the two groups are greater than would be expected by chance; there is a statistically significant difference (P = <0.001)

H&E total area of lesion

t-test   Tuesday, February 28, 2006, 17:05:31

Data source: Data 1 in Notebook

Normality Test: Passed (P = 0.470)

Equal Variance Test: Failed (P = 0.029)

Test execution ended by user request, Rank Sum Test begun

Mann-Whitney Rank Sum Test   Tuesday, February 28, 2006, 17:05:31

Data source: Data 1 in Notebook

Group N   Missing
Col 5   5   0
Col 6   5   0

Group Median   25%   75%
Col 5   133881.000   133430.800   134563.575
Col 6   28566.630   28544.090   28805.165

T = 40.000 n(small)= 5 n(big)= 5 P(est.)= 0.012 P(exact)= 0.008

The differences in the median values among the two groups are greater than would be expected by chance; there is a statistically significant difference (P = 0.008)

IHC Max depth

t-test   Tuesday, February 28, 2006, 17:07:52

Data source: Data 1 in Notebook

Normality Test: Passed (P = 0.397)

Equal Variance Test: Passed (P = 0.055)

Group N   Missing
Col 9   10   0
Col 10 10   0

Group Mean   Std Dev   SEM
Col 9   581.145   7.130 2.255
Col 10 334.955   2.758   0.872

Difference   246.190

t = 101.829 with 18 degrees of freedom. (P = <0.001)

 95 percent confidence interval for difference of means: 241.110 to 251.269

The difference in the mean values of the two groups is greater than would be expected by chance; there is a statistically significant difference between the input groups (P = <0.001).

Power of performed test with alpha = 0.050: 1.000

IHC Max Diameter

t-test   Tuesday, February 28, 2006, 17:10:34

Data source: Data 1 in Notebook

Normality Test: Failed (P = 0.047)

Test execution ended by user request, Rank Sum Test begun

Mann-Whitney Rank Sum Test   Tuesday, February 28, 2006, 17:10:34

Data source: Data 1 in Notebook

Group N   Missing
Col 11 10   0
Col 12 10   0

Group Median   25%   75%
Col 11 468.795   468.137   480.397
Col 12 145.675   144.673   146.234

T = 155.000 n(small)= 10 n(big)= 10 (P = <0.001)

The differences in the median values among the two groups are greater than would be expected by chance; there is a statistically significant difference (P = <0.001)

IHC total Area

t-test   Tuesday, February 28, 2006, 17:13:02

Data source: Data 1 in Notebook

Normality Test: Passed (P = 0.086)

Equal Variance Test: Passed (P = 0.061)

Group N   Missing
Col 13 5   0
Col 14 5   0

Group Mean   Std Dev   SEM
Col 13 48666.386   1370.122   612.737
Col 14 28867.358   299.299   133.851

Difference   19799.028

t = 31.568 with 8 degrees of freedom. (P = <0.001)

 95 percent confidence interval for difference of means: 18352.733 to 21245.323

The difference in the mean values of the two groups is greater than would be expected by chance; there is a statistically significant difference between the input groups (P = <0.001).

Power of performed test with alpha = 0.050: 1.000

T test comparing H&E data and IHC data for total area of ms lesion

t-test   Wednesday, March 01, 2006, 14:57:15

Data source: Data 1 in Notebook

Normality Test: Passed (P = 0.558)

Equal Variance Test: Passed (P = 0.285)

Group N   Missing
Col 4   5   0
Col 5   5   0

Group Mean   Std Dev   SEM
Col 4   133961.180   744.294   332.859
Col 5   48666.386   1370.122   612.737

Difference   85294.794

t = 122.320 with 8 degrees of freedom. (P = <0.001)

 95 percent confidence interval for difference of means: 83686.793 to 86902.795

The difference in the mean values of the two groups is greater than would be expected by chance; there is a statistically significant difference between the input groups (P = <0.001).

Power of performed test with alpha = 0.050: 1.000

T test comparing H&E data and IHC data for total area of ns lesion

t-test   Wednesday, March 01, 2006, 15:00:59

Data source: Data 1 in Notebook

Normality Test: Passed (P = 0.221)

Equal Variance Test: Passed (P = 0.448)

Group N   Missing
Col 7   5   0
Col 8   5   0

Group Mean   Std Dev   SEM
Col 7   28670.418   197.586   88.363
Col 8   28867.358   299.299   133.851

Difference   -196.940

t = -1.228 with 8 degrees of freedom. (P = 0.254)

 95 percent confidence interval for difference of means: -566.793 to 172.913

The difference in the mean values of the two groups is not great enough to reject the possibility that the difference is due to random sampling variability. There is not a statistically significant difference between the input groups (P = 0.254).

Power of performed test with alpha = 0.050: 0.093

The power of the performed test (0.093) is below the desired power of 0.800. You should interpret the negative findings cautiously.